Active fault mapping in Tairāwhiti Gisborne District using LiDAR data

NJ Litchfield
DB Townsend
A Howell
R Morgenstern

GNS Science Consultancy Report 2022/119
November 2022

DISCLAIMER

This report has been prepared by the Institute of Geological and Nuclear Sciences Limited (GNS Science) exclusively for and under contract to Gisborne District Council. Unless otherwise agreed in writing by GNS Science, GNS Science accepts no responsibility for any use of or reliance on any contents of this report by any person other than Gisborne District Council and shall not be liable to any person other than Gisborne District Council, on any ground, for any loss, damage or expense arising from such use or reliance.

Use of Data:

Date that GNS Science can use associated data: November 2022

BIBLIOGRAPHIC REFERENCE

Litchfield NJ, Howell A, Townsend DB, Morgenstern R. 2022. Active fault mapping in Tairāwhiti Gisborne District using LiDAR data. Lower Hutt (NZ): GNS Science. 56 p. Consultancy Report 2022/119.

CONTENTS

FIGURES

TABLES

APPENDICES

APPENDIX FIGURES

APPENDIX TABLES

EXECUTIVE SUMMARY

Tairāwhiti Gisborne District lies within the northern part of the Hikurangi Subduction Zone, and it is important to understand the risk of large earthquakes that may occur on active faults in the district. In Aotearoa New Zealand, the ground-surface rupture hazard posed by an active fault is largely characterised by constraining its location at the ground surface and defining its level of activity (that is, its recurrence interval of surface rupture).

Only a few active faults have previously been mapped in Tairāwhiti Gisborne District, and no systematic mapping has been undertaken since 2000. Recently obtained (2018–2020) Light Detection and Ranging (LiDAR) data provided an opportunity to trial a semi-automated fault-mapping tool alongside traditional manual methods to map faults at a scale suitable for land-use planning purposes. Gisborne District Council commissioned GNS Science to provide updated GIS-based active fault location data, Fault Avoidance Zones (FAZs) and Fault Awareness Areas (FAAs) for specific areas near towns and critical infrastructure and around known active faults within Tairāwhiti Gisborne District.

A trial was undertaken of a semi-automated fault-mapping tool (edge-detection algorithms) on selected faults using the LiDAR data. In general, the tool was unsuccessful, primarily due to the steep topography and the relatively subtle topographic expressions of many of the faults in Tairāwhiti Gisborne District. Although the success of this tool can be improved by choosing parameters that work well for individual sites, these parameters will vary widely from site to site, meaning that it is not possible to readily scale up this tool for use across the whole district. Nevertheless, the trial was useful to understand these limitations, and several recommendations are made for future tool development.

The new manual mapping using LiDAR data identified a number of traces along many of the previously mapped faults and some new faults. In general, the faults are short (≤11 km in length) and scattered throughout Tairāwhiti Gisborne District, although the most continuous new faults are concentrated in the west and south. Most are inferred to be normal faults, and the overall short lengths support previous interpretations that they are secondary faults. New possible active fault traces have been mapped crossing Tolaga Bay town, near Tokomaru Bay town, east of Ruatoria and crossing the water supply reservoirs. Active fault traces were not identified along five previously mapped faults, the Motu, Kotare, Pangopango, Arakihi and Otoko-Totangi faults, and so these have now been removed from the active fault dataset.

Recurrence interval (RI) information is only available for two faults in Tairāwhiti Gisborne District, the Repongaere and Pakarae faults, which have been assigned to RI Classes III (>3500 to ≤5000 years) and II (>2000 to ≤3500 years), respectively, with medium confidence. FAZs have been developed for these faults following the methodology outlined in the Ministry for the Environment (MfE) Active Fault Guidelines. FAAs have been developed for the remaining faults by buffering the traces by 125 m either side (total width 250 m).

We recommend that the FAZs and FAAs developed in this study be used to inform future planning decisions and to replace any existing active fault datasets. We also recommend further work that could be undertaken to investigate the tectonic origin and RI Class of newly identified faults in the vicinity of Tolaga Bay, Tokomaru Bay, Ruatoria and the water supply reservoirs. This could be achieved through a combination of field mapping, geophysical surveys (e.g. ground-penetrating radar) and/or paleoseismic trenching studies.

1.0 INTRODUCTION

1.1 Background and Context

Aotearoa New Zealand lies within the deforming boundary zone between the Australian and Pacific tectonic plates (Figure 1.1a). The plate boundary zone is made up of three major components – the Hikurangi Subduction Zone, the Alpine Fault and the Puysegur Subduction Zone. The area administered by Te Kaunihera o Te Tairāwhiti Gisborne District Council (hereafter referred to as Tairāwhiti Gisborne District) lies within the northern part of the Hikurangi Subduction Zone, where the Pacific Plate is being forced (subducted) beneath the Australian Plate at the Hikurangi Trough, which lies 70–120 km offshore of the east coast. The rate of movement between the Australian and Pacific plates is high in this area (50–60 mm/yr; Wallace et al. 2012), and Tairāwhiti Gisborne District has experienced a significant number of magnitude 5 and 6 earthquakes since 1940 and seven infrastructure-damaging earthquakes since 1960 (Figure 1.1b). It is therefore important to understand the risk of large earthquakes that may occur on active faults in the district.

Only a few active faults have been mapped previously in Tairāwhiti Gisborne District (Figures 1.1b and 1.2), and no systematic mapping has been undertaken since the publication of the 1:250,000-scale geological map in 2000 (Mazengarb and Speden 2000).[1] The sparse, short, previously mapped active faults have often been considered minor, shallow, secondary faults rupturing in response to rapid uplift of the Raukumara Peninsula, driven by movement on the Hikurangi Subduction Zone (Thornley 1996; Litchfield et al. 2007; Berryman et al. 2009). However, Tairāwhiti Gisborne District is also subject to high rates of fluvial and landslide erosion (e.g. Gage and Black 1979; Hicks et al. 1996; Marden et al. 2008, 2018), which has made identification of active faults challenging, so it has long been suspected that there are more active faults than previously mapped.

Recently (2018–2020), Light Detection and Ranging (LiDAR) data have been obtained covering Tairāwhiti Gisborne District. Regional LiDAR data are obtained from fixed-wing aircraft surveys and are used to produce very detailed (metre-scale) models of the earth surface with the vegetation removed. The ability to see the ground surface at high resolution (~1 m) has revolutionised active fault mapping, which is being revised across much of Aotearoa New Zealand as a result. LiDAR has also provided suitable data to develop semi-automated active-fault-mapping tools, and the preliminary results from the application of these in Tairāwhiti Gisborne District are also presented here.

1 The far southwestern corner of Tairāwhiti Gisborne District is in the area mapped by Leonard et al. (2010) (QMAP Rotorua), but no active faults were mapped within the district.

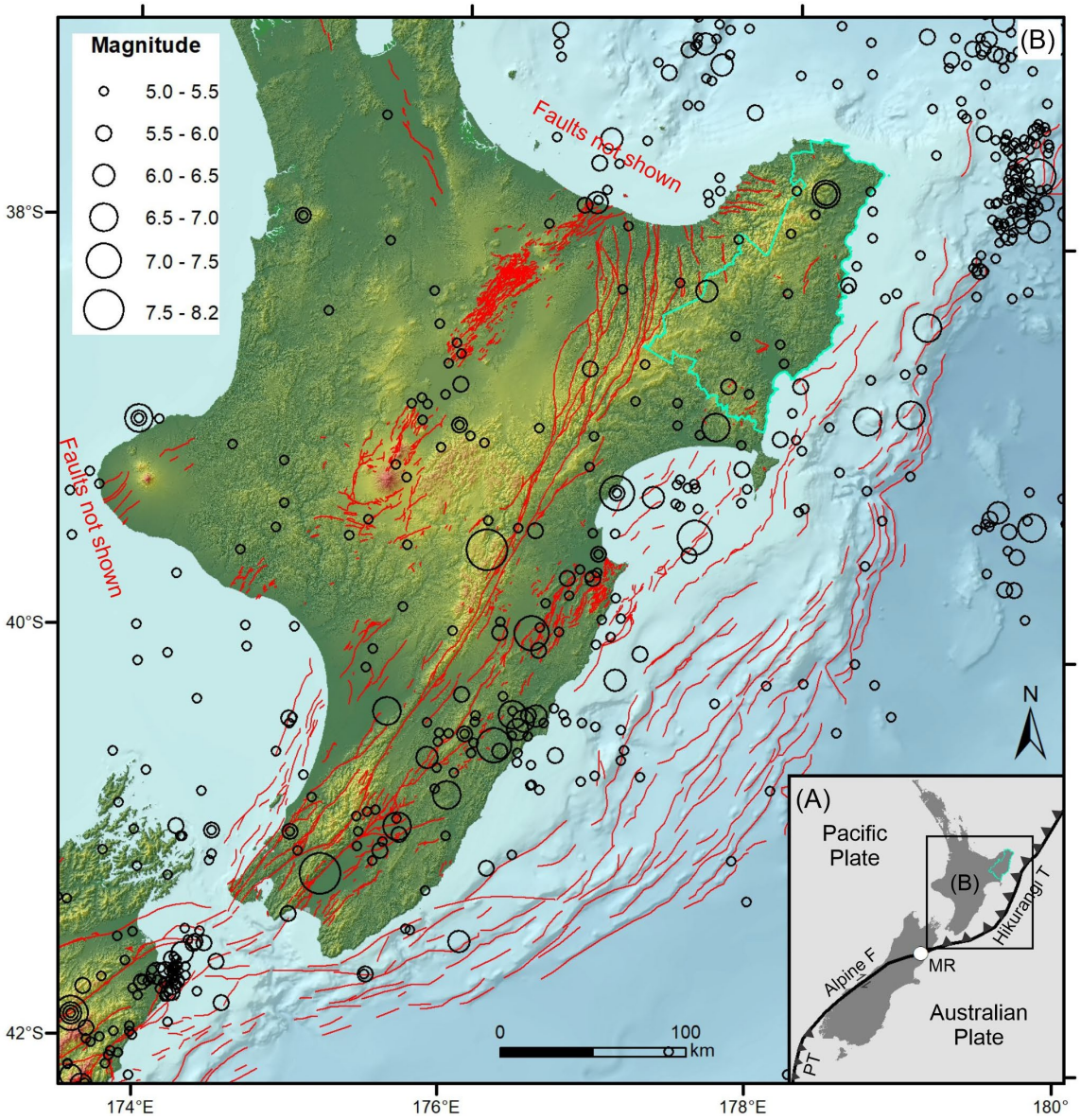

Figure 1.1 Tectonic setting of Tairāwhiti Gisborne District (outlined in bright green). (a) Plate boundary zone. F is fault, MR is the Mason River site (referred to in Section 2.1.2), PT is Puysegur Trench, T is Trough. (b) Active faults (red lines) and historical earthquakes (circles scaled according to magnitude). Onshore active faults are previously mapped (i.e. prior to this study) from the 1:250,000-scale New Zealand Active Fault Database (https://data.gns.cri.nz/af/; Langridge et al. 2016). Selected offshore active faults are from Barnes (1994), Barnes and Audru (1999), Barnes et al. (2002, 2010), Mountjoy and Barnes (2011), Mountjoy et al. (2009), Pondard and Barnes (2010) and Nodder et al. (2007). Earthquake epicentres are shallow (≤40 km) historical (post-1840 AD) earthquakes from the GeoNet earthquake catalogue (https://quakesearch.geonet.org.nz/).

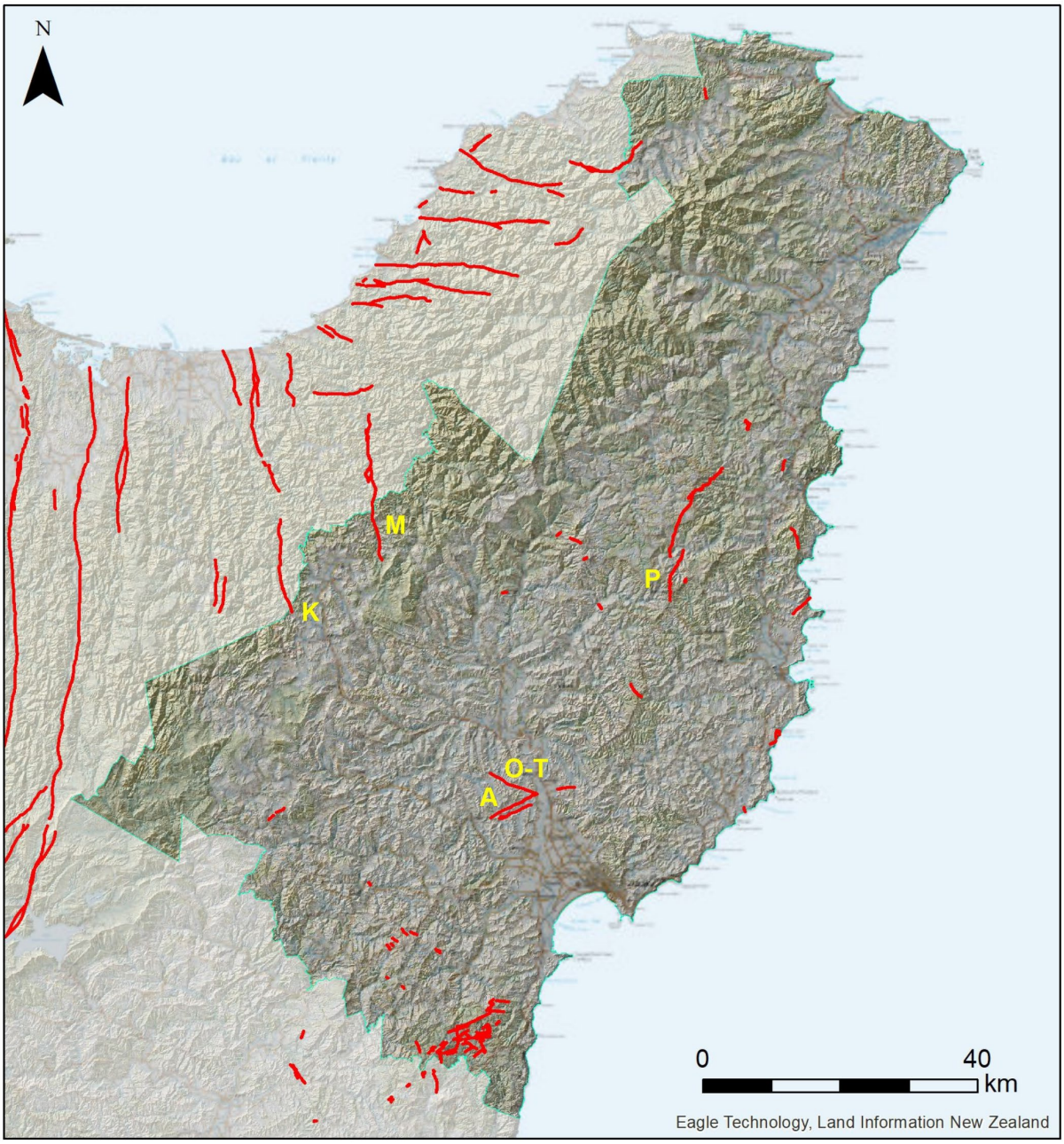

Figure 1.2 Previously mapped onshore active faults in Tairāwhiti Gisborne District. Red lines denote active faults and dark shading denotes the district. These are from the high-resolution version of the New Zealand Active Faults Database (Jongens and Dellow 2003), but, in the district, most are from 1:50,000-scale mapping compiled by Mazengarb and Speden (2000). Yellow labels are selected faults referred to in the text – A is the Arakihi Fault, K is the Kotare Fault, M is the Motu Fault, O-T is the Otoki-Totangi Fault, P is the Pangopango Fault.

1.2 Objectives and Scope

Te Kaunihera o Te Tairāwhiti Gisborne District Council commissioned GNS Science to provide updated GIS-based active fault location data, Fault Avoidance Zones (FAZs) and Fault Awareness Areas (FAAs) for specific areas within the district. The specific project tasks were to:

1. Use available high-resolution LiDAR data to investigate active fault traces in priority areas described below and shown in Figure 1.3:
    - **Priority 1**: Areas proximal to the following towns and plains (shown in black in Figure 1.3): Gisborne City, Tolaga Bay, Tokomaru Bay, Ruatoria and Te Araroa.

- **Priority 2**: Main roading corridors, selected critical water supply network infrastructure and known active faults (each buffered by 3 km and shown in blue in Figure 1.3).
- **Priority 3**: Wider area of interest identified by Gisborne District Council (shown in yellow in Figure 1.3). Due to the scale and terrain, less time will be devoted to priority 3 areas compared to priority 1 and 2 areas. Prototype active fault mapping semi-automated tools will be tested and used to help locate faults within the priority 3 areas (and outside of priority 3 if time/budget allows).

2. Develop FAZs or FAAs as appropriate for any faults identified.
3. Review recurrence intervals and attribute information for identified active faults where applicable.

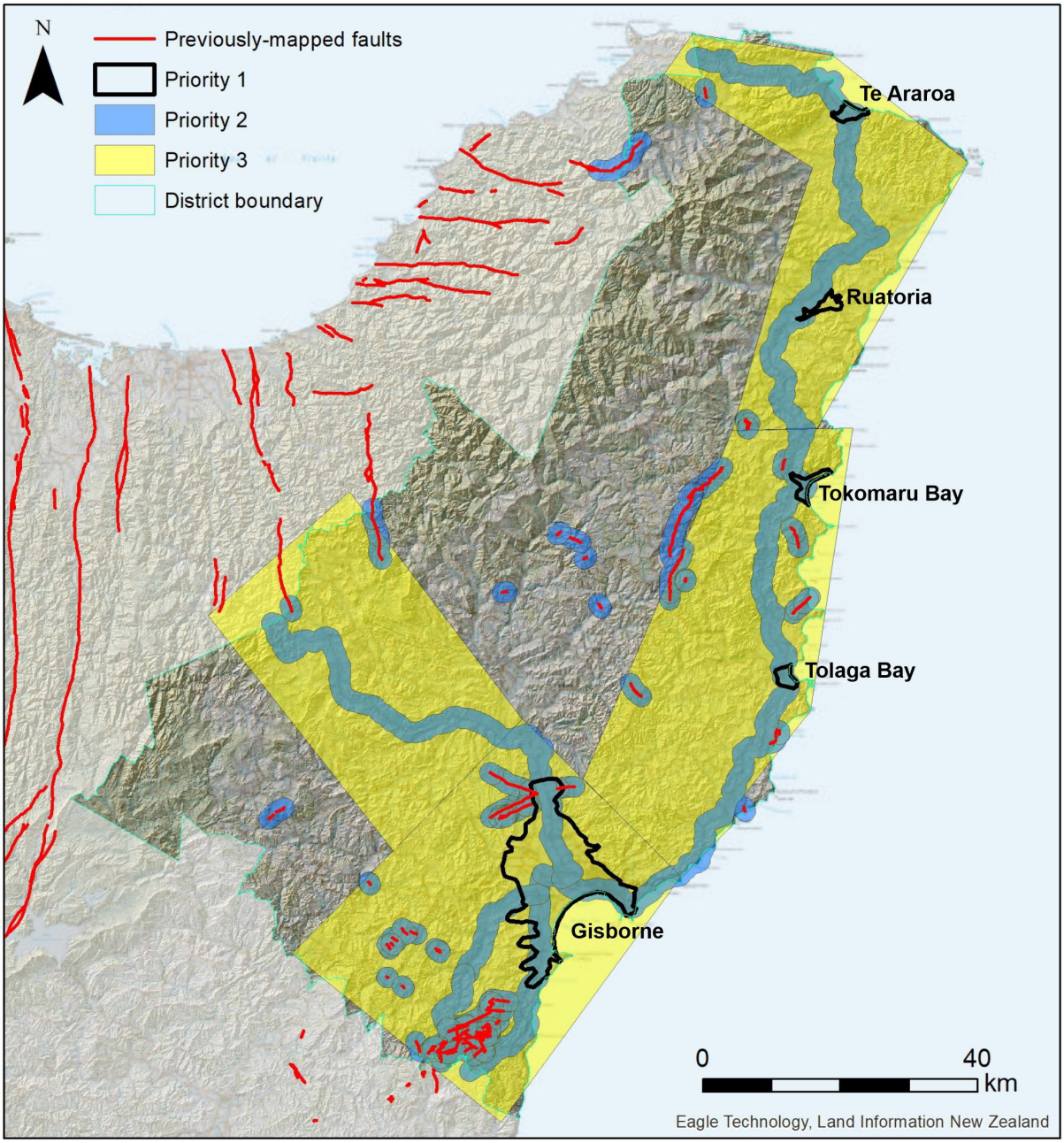

Figure 1.3 Fault mapping priority 1, 2 and 3 areas in Tairāwhiti Gisborne District. Priority 1 areas are towns (labelled); priority 2 areas are main roading corridors, selected critical water-supply network infrastructure and previously mapped faults; and priority 3 areas are wider areas of interest identified by Gisborne District Council.

1.3 Fault Avoidance Zones and Fault Awareness Areas for District Plan Purposes

Ground-surface rupture hazard is the permanent breakage and buckling of the ground along an active fault (see Appendix 1 for definitions and descriptions of types of active faults) during an earthquake, which can cause considerable damage to any infrastructure upon or crossing the fault. However, compared with earthquake shaking, which can be widespread, the likely location of ground-surface rupture hazard can often be located accurately to within a few metres, so potential damage to built structures can often be mitigated through avoidance. Risk-based land-use planning tools have been developed for this purpose, and these include the two land-use planning tools used in this study, FAZs and FAAs, which are summarised below.

1.3.1 Fault Avoidance Zones Overview

FAZs are a recommended risk-based tool to mitigate surface-rupture hazard for land-use planning purposes, as described in the Ministry for the Environment (MfE) Active Fault Guidelines (Kerr et al. 2003). The aim of the MfE Active Fault Guidelines is to assist resource-management planners tasked with formulating land-use policy and making decisions about development of land on, or near, active faults. The MfE Active Fault Guidelines provide information about active faults, specifically fault-rupture hazard, and promote a risk-based approach when dealing with development in areas subject to ground-surface fault-rupture hazard. In the MfE Active Fault Guidelines, the surface-rupture hazard of an active fault at a specific site is characterised by two parameters:

1. The **location/complexity** of surface rupture of the fault.
2. The activity of the fault, as measured by its average **recurrence interval** of surface rupture.

The MfE Active Fault Guidelines also advance a hierarchical relationship between fault recurrence interval and building importance, such that the greater the importance of a structure with respect to life safety, the longer the recurrence interval of the fault required before a plan should enable construction. For example, only low-occupancy structures, such as farm sheds and fences (i.e. Building Importance Category [BIC] 1 structures), should be allowed to be built across active faults with average recurrence intervals of surface rupture less than 2000 years (i.e. RI Class I).

In practise, FAZs are created by defining fault complexity zones, which define the likely rupture zone of active faults, and then adding a 20 m setback buffer. The fault complexity zones are themselves generated from buffers surrounding the detailed fault mapping linework, with the width of fault complexity zones generally determined by an expert assessment of fault characteristics and location accuracy, as well as accounting for the resolution and georeferencing uncertainty of the data.

In this study, FAZs have only been developed for two faults for which recurrence interval can be estimated. Details on how these FAZs were constructed are contained in Section 3.3.

1.3.2 Fault Awareness Areas Overview

FAAs were originally developed for districts within the Canterbury region from 1:250,000-scale fault maps produced for each district (e.g. Barrell and Townsend 2012; Barrell 2013). The purpose of FAAs was *to show the general location of active faults and thereby highlight areas where a potential fault-rupture hazard may be present and where future work should*

be undertaken. FAAs were created by a single buffer of ±125 m or ±250 m (depending on fault certainty and surface form) either side of mapped active faults (total widths 250 m or 500 m, respectively). Guidelines for the use of FAAs for planning purposes in the Canterbury region were developed by Barrell et al. (2015).

Subsequent to the Canterbury region fault mapping, FAAs have been developed for several other local authorities and at a variety of scales (e.g. Barrell 2019; Litchfield et al. 2020b, 2022; Langridge et al. 2021). The use of FAAs has become a practical way to efficiently map faults in areas without LiDAR data, for planning purposes in lower-priority areas, or for faults with no recurrence interval information.

FAAs have been developed for the majority of faults mapped in this study due to the lack of recurrence interval information. A description of how the FAAs were created is contained in Section 3.4.

1.4 Report Contents and Layout

This report summarises the results of this project and describes the active fault (GIS) map data provided.

- Section 2 describes a trial of a semi-automated tool to map active faults using the LiDAR data.
- Section 3 outlines the methodology for manual active fault mapping and developing FAZs and FAAs.
- Section 4 describes the manual mapping results for each of the towns (priority 1); previously mapped active faults (priority 2) and new faults; and remaining faults, including that cross critical infrastructure (priority 2 and 3).
- Section 5 provides recommendations for use of the information in this report and future work.

2.0 SEMI-AUTOMATED FAULT-MAPPING TOOL TRIAL

Mapping of fault traces for the definition of FAZs and FAAs is of crucial importance for understanding hazards associated with future fault rupture (as discussed in Section 1). Despite this importance, mapping faults using conventional methods (e.g. Clark and Ries 2016; Langridge and Morgenstern 2019; Litchfield et al. 2020b, 2022) is a time-consuming process, especially in regions with extensive LiDAR coverage; in such regions, the availability of high-resolution elevation data means that there are significantly more terrain features that must be checked manually when searching for faults. As a result, any computational tool that automates part (or all) of the fault-mapping process is potentially very useful, as it may lead to significant reductions in the time and cost associated with fault mapping.

In this section, we discuss the trial of a tool to assist earthquake geologists with fault mapping, based on the edge detection algorithm of Canny (1986). This tool is intended to streamline rather than replace manual mapping: differences between faults and other geomorphic features like terrace risers are often subtle, so that, in many cases, expert judgement will be required to confirm whether the mapped feature is a fault. We first discuss the basis for the tool (Section 2.1) and then illustrate its potential using case studies from two relatively simple geomorphic settings: part of the San Andreas Fault in California (Section 2.1.1) and the Hope Fault in North Canterbury (Section 2.1.2). Next, we discuss the attempted application of the tool in Tairāwhiti Gisborne District (Section 2.2), identifying limitations when the tool is used in regions with steep topography. Finally, we make recommendations concerning the future development and use of semi-automated fault-mapping tools to aid fault mapping in Tairāwhiti Gisborne District and other areas (Section 2.3).

2.1 Edge-Detection Algorithms as a Tool to Assist Manual Fault Identification

The possible use of edge-detection algorithms to map active tectonic faults relies on the fact that active fault traces are often sharp, linear features that cut across topography for hundreds of metres or kilometres. An example of a clear fault scarp illuminated by LiDAR data is shown in Figure 2.1.

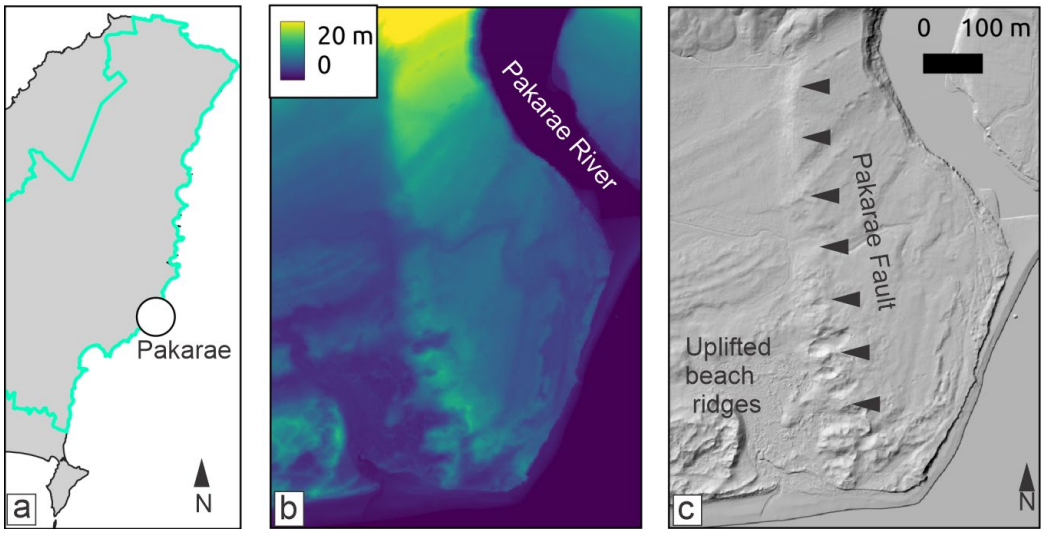

Figure 2.1 LiDAR representation of a fault scarp at Pakarae River mouth (Pakarae Fault). (a) Location of the Pakarae River mouth relative to the rest of Tairāwhiti Gisborne District (outlined in bright green), (b) a digital elevation model of the site derived from LiDAR data; and (c) a LiDAR hillshade model illuminated from the northwest, with the top of the Pakarae Fault scarp marked by black triangles. Uplifted beach ridges are also visible to the west of the scarp, and dunes obscure much of the terrain in the south.

Edge detection works by identifying regions in an image where there are steep gradients between pixel values (Canny 1986). In the context of a LiDAR Digital Elevation Model (DEM), these gradients are identical to topographic gradients. The application of the Canny edge detector to a LiDAR DEM involves four main steps:

1. Normalising the DEM to a greyscale image by assigning each pixel a value between 0 and 255.
2. Applying a Gaussian filter to smooth the image slightly and filter out noise on short wavelengths of a few pixels. As we are typically using LiDAR DEMs with pixel sizes of 1 m and looking for fault traces that are hundreds or thousands of metres long, this step is especially useful for our purposes.
3. Calculating the intensity gradient (similar to slope) of the smoothed image.
4. Removing gradient values below a specified threshold by setting the values of those pixels to zero. This step simplifies the image by removing smooth (low gradient) areas that are unlikely to represent edges. At present, we choose this threshold on a trial-and-error basis to determine the most suitable value for a region of interest.

These steps are followed by further post-processing to reduce noise (Canny 1986; Bradski and Kaehler 2008), but we do not discuss the post-processing here.

We modify the outputs of the edge-detection algorithm to assist in fault identification through two additional steps. First, we apply a maximum filter over either a 3 x 3 pixel or 5 x 5 pixel moving window to amplify and thicken edges and make possible faults appear more prominent. Second, we apply a Hough line transform algorithm (Hough 1959; Duda and Hart 1972) to identify straight lines above a certain length, as fault traces are likely to be relatively straight, at least over ~50 m length scales. The edge-detection results and the lines identified using the Hough line transform algorithm are intended to be used either together or separately to guide manual interpretations of geomorphic features that may be faults. Note that the lines identified by the Hough line transform algorithm do not need to be continuous; it is possible to specify a maximum gap below which segments are treated as part of the same line, as well as a minimum length for mapped line segments.

2.1.1 Example 1: San Andreas Fault at Wallace Creek

Tairāwhiti Gisborne District is a challenging area in which to develop and test a new fault-mapping tool, mainly due to high erosion rates and slow fault slip rates (at least compared with many other tectonically deforming areas). These factors mean that the geomorphic expression of faulting is not as clear in Tairāwhiti Gisborne District as it would be in regions with lower rainfall and faster fault slip rates. Before describing the application of our tool to the more complex terrain of Tairāwhiti Gisborne District, we demonstrate its performance in simpler geomorphic settings.

Our first example is a section of the San Andreas Fault where it crosses the Carrizo Plain at Wallace Creek, California, USA. The Carrizo Plain is semi-arid (annual rainfall ~230 mm[2]), and the slip rate of the San Andreas Fault there is 33.9 ± 2.9 mm/year (Grant Ludwig et al. 2019), which leads to exceptional preservation of the fault scarp. This location was previously used by Sare and Hilley (2018) to test Scarplet, a tool they developed for detecting and dating of fault scarps.

2 https://www.blm.gov/programs/national-conservation-lands/california/carrizo-plain-national-monument

Figure 2.2 shows the successful application of our tool at this site. The results of the edge-detection component of the algorithm illuminate the fault trace (Figure 2.2b), as well as a road on the western side of the fault and deeply incised stream valleys in the hanging-wall (east) side. As, in this instance, the fault trace is the longest, straightest line in the edge-detection outputs, it is relatively easy to map it using a Hough line transform (Figure 2.2c). Note that to identify only the fault trace, it is necessary to either: (1) specify a minimum length greater than 500 m for mapped lines or (2) specify a N–S orientation for mapped lines. However, specifying such parameters is only appropriate for areas with long, straight fault segments or where the strike of likely fault segments is known prior to mapping.

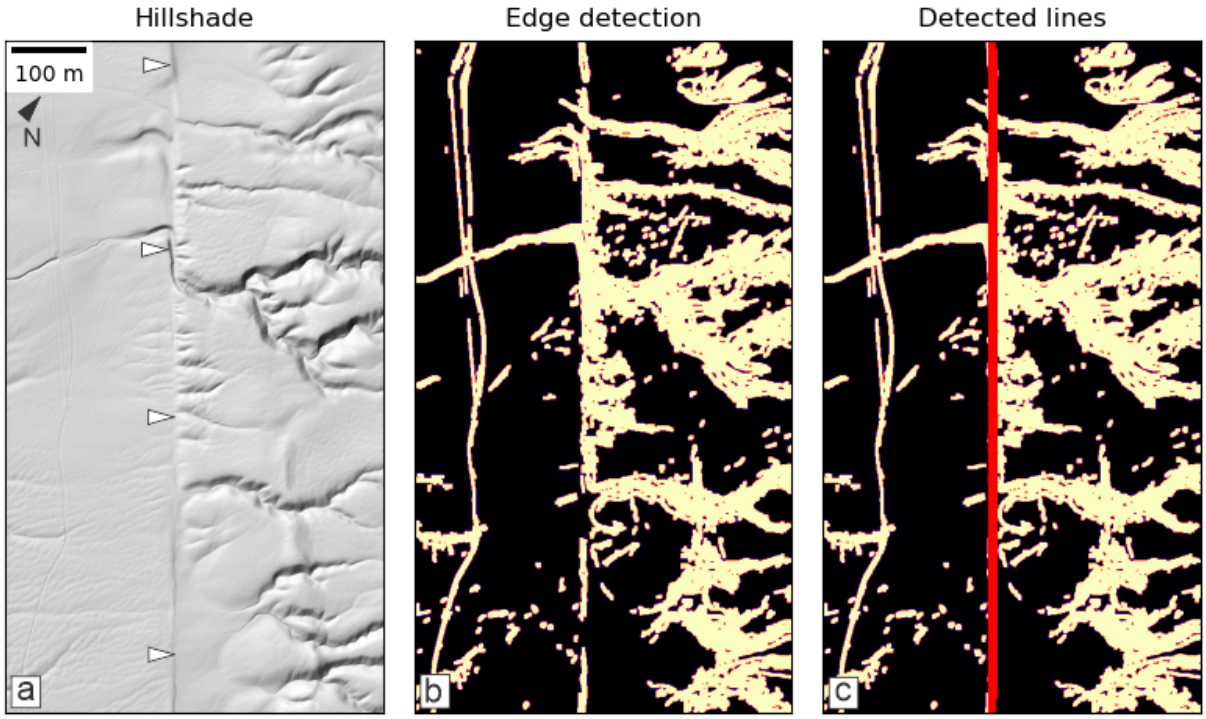

Figure 2.2 Application of our edge-detection tool to the San Andreas Fault at Wallace Creek, California, USA. Note that we do not provide a location map for this site, due to the large distance from Tairāwhiti Gisborne District. (a) LiDAR hillshade of the site (NCALM 2006). The trace of the San Andreas Fault is marked by small white triangles. (b) Outputs of the edge-detection component of our methodology, including the maximum-filter post-processing step. Lighter colours represent clearly detected edges in the topography. (c) Line fitted automatically to the edge-detection results using a Hough line transform. This line follows the scarp of the San Andreas Fault very closely.

2.1.2 Example 2: Hope Fault at Mason River

The main advantage of using the San Andreas Fault at Wallace Creek as a case study is that it has a fault trace that is clearly expressed in the landscape and is geometrically simple. However, most fault traces in Aotearoa New Zealand and worldwide are more sinuous, less continuous and less well expressed than the Wallace Creek example. To test the efficacy of our method on fault traces that are more challenging to map, we now apply it to a more complex geomorphic setting. Our chosen site is the Hope Fault at Mason River, North Canterbury, Aotearoa New Zealand (see Figure 1.1a for location), where two main traces of the Hope Fault cut across fluvial terraces (Figure 2.3a; Beauprêtre et al. 2012).

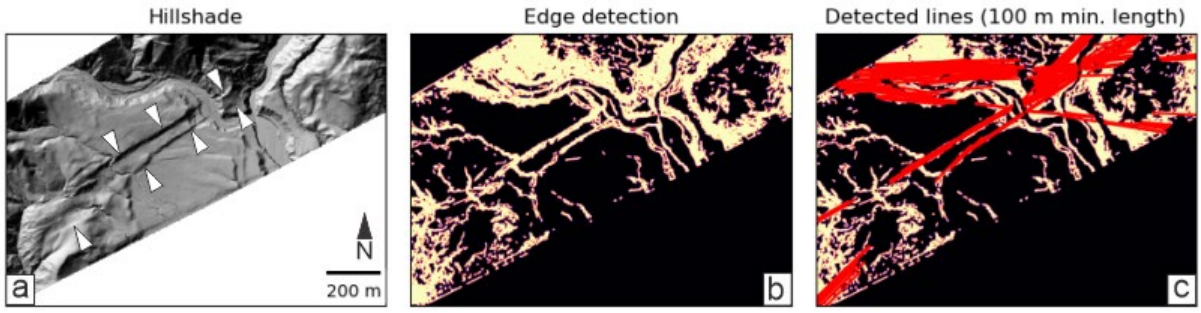

Figure 2.3 Application of our edge-detection tool to the Hope Fault at Mason River, North Canterbury (location shown on Figure 1.1a). (a) LiDAR hillshade of the site (ANR 2018). Major and selected traces of the Hope Fault are marked by white triangles. (b) Outputs of the edge-detection component of our methodology, including the maximum-filter post-processing step. (c) Lines fitted automatically to the edge-detection results using a Hough line transform, with a minimum line length of 100 m.

Our edge-detection tool is successful at illuminating the Hope Fault traces where they cut the sub-horizontal river traces (Figure 2.3b) but is much less effective in areas of steeper, rougher topography. The riverbanks and much of the hillier terrain in the southwest of the site are highlighted as edges by the tool. When a Hough line transform is applied (with a 100 m minimum line length), lines corresponding to the manually identified traces in Figure 2.3a are generated (red lines in Figure 2.3c). However, many of the red lines in Figure 2.3c follow fluvial features rather than fault traces. As a consequence, we rate this application of the tool as less successful than the San Andreas Fault example. Nonetheless, the edge-detection tool is successful at identifying the main fault Hope Fault traces, and this example highlights that areas of complex terrain would require detailed manual inspection.

2.2 Application to Tairāwhiti Gisborne District

The main purpose of this section is to assess the suitability of our edge-detection tool to support manual fault mapping in Tairāwhiti Gisborne District. In general, our attempts to use it in the district were unsuccessful, primarily due to the steep topography throughout the district and the relatively subtle topographic expressions of many of the faults. We will describe results from use of the tool to map part of the Smart Road fault. The Smart Road fault results will be followed by a more general discussion of the limited success of our tool in Tairāwhiti Gisborne District.

2.2.1 Application to the Smart Road Fault

The Smart Road fault is represented by a series of traces in western Tairāwhiti Gisborne District (Figure 2.4a), newly identified from LiDAR data during the manual mapping component of this project (further discussion in Section 4). The fault appears to accommodate a predominantly normal sense of movement and has been chosen to test our tool because of a significant number of scarps that are clearly visible in the LiDAR DEM (Figure 2.4d).

We applied our edge-detection tool to a 600 x 500 m area around the Smart Road fault, chosen due to the clear expression of the fault scarps there. Figure 2.4c shows the results of edge detection applied to the area; Figure 2.4b and 2.4e allow a comparison between manual mapping and the results from a Hough line transform of the edge-detection outputs. Our automated tool identifies ~50% of the manually mapped faults, although not as accurately. Importantly, some of the manually mapped faults are not visible in the edge-detection outputs. This absence is problematic because it represents a crucial limitation of the tool. If all of the manually mapped faults appeared in the edge-detection outputs, together with additional features not related to faulting, then it might theoretically be possible to limit manual

involvement to a review of the edge-detection outputs, saving time. However, as the algorithm currently misses some faults, for a robust assessment of an area for active faulting it remains necessary to review the LiDAR DEM manually. In this case, and with the available LiDAR data, the edge-detection tool does not save much (if any) time relative to manual mapping.

Another limitation of the tool in this setting is a tendency to identify ridgelines and roads or tracks as edges (and therefore possible faults). This limitation is similar to the problems caused by the riverbanks in the Mason River (Hope Fault) example (Section 2.1.2) but is less important than the edge-detection algorithm not identifying some fault scarps.

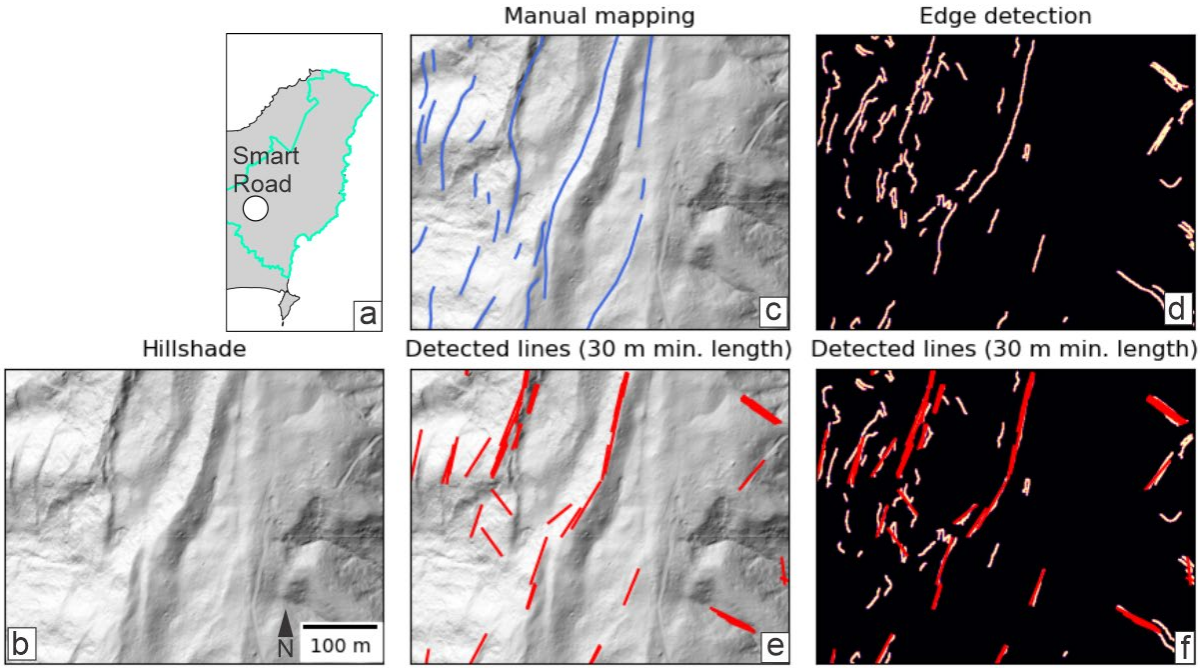

Figure 2.4 Application of our edge-detection tool to the Smart Road fault in western Tairāwhiti Gisborne District. (a) Approximate location of (b)–(f) relative to the rest of the district (boundary shown in bright green). (b) Uninterpreted LiDAR hillshade model. (c) LiDAR hillshade of a selected small area with manually mapped fault traces in blue; manual mapping of these traces is discussed further in Section 4. (d) Results of our edge-detection algorithm for the site in (b). (e) LiDAR hillshade model with lines detected by applying a Hough line transform to our edge-detection results (minimum line length 30 m). (f) The same lines as in (e), plotted over the edge-detection results in (c).

2.2.2 General Limitations for Use of the Edge-Detection Tool in Tairāwhiti Gisborne District

Other than the limitations described above, the main challenge with the edge-detection tool is scaling its use to the whole Tairāwhiti Gisborne District. Although we can choose values for parameters that make the tool work well for individual sites, these parameters will vary widely from site to site. Most importantly, the threshold value chosen for the Canny Edge Detection algorithm has a very strong influence on results, and the optimal threshold varies by an order of magnitude between sites (including the three examples presented here). For edge detection to work on the scale of a whole district, it will be necessary to optimise this parameter in a less time-consuming manner than the trial-and-error approach that we have tested here.

2.3 Recommendations for Future Development of Semi-Automated Fault-Mapping Tools

Our trial of a new edge-detection tool has demonstrated the clear potential of semi-automated techniques to support expert judgement during fault mapping. However, this trial has also identified several weaknesses of our tool that probably also apply to other semi-automated fault-mapping techniques. We now discuss possible improvements that could be made to our edge-detection tool, as well as the likely advantages and disadvantages of alternative semi-automatic techniques that could be applied instead.

2.3.1 Possible Improvements to the Edge-Detection Tool

There are several possible modifications to our methodology that could improve its ability to identify faults in Tairāwhiti Gisborne District and other areas with complex topography. One possible approach would be to mask ridgelines, deeply incised river valleys and any previously mapped landslides from the LiDAR dataset so that they do not influence edge-detection results. The removal of these terrain features from the data analysed by the semi-automatic tool would allow the tool to focus on terrain where it performs better, possibly improving results. In such a case, the masked areas would need to be examined manually to look for faults.

A second possible improvement would be to develop ways to automatically adjust the threshold value used by the Canny Edge Detection algorithm. At present, we adjust this threshold using a trial-and-error approach for each site, which restricts the applicability of our tool over a large area. It might be possible to adjust the threshold to optimise the density of edge-detection outputs – for example, raise the threshold if the outputs identify more than a desired number of edges. Alternatively, the trial-and-error approach could be applied to a wide variety of sites to create a training dataset for a machine-learning algorithm that could then adjust thresholds automatically based on parameters like terrain roughness.

Finally, a scale-dependent implementation of the edge-detection tool might allow information about large-scale tectonic features to guide smaller-scale mapping. This approach might also allow the filtering out of short-wavelength terrain roughness, which manifests as noise in the edge-detection results.

2.3.2 Possible Alternative Approaches

The semi-automated mapping of fault scarps is an area of significant research interest worldwide, with two new methods published since 2021 (Mattéo et al. 2021; Scott et al. 2022). Both of these tools utilise deep-learning-based methodologies and show promising results. However, they have only been trained on data from relatively simple settings; like our tool, these methods are unlikely to perform well in complex terrain like that of Tairāwhiti Gisborne District, although they may still be worth trialling there. This lack of training data was the main reason for our adoption of the edge-detection approach, which offers more scope for manual tuning but also clearly has limitations. As this relatively new field develops, it is likely that datasets from areas with steeper terrain and more subtle fault expressions will be used to train algorithms, which may improve algorithm mapping performance. However, development of such algorithms will be technically challenging and time-consuming. In the immediate future – and probably for several years to come at least – it is likely that manual mapping will remain the best way to identify fault traces in Tairāwhiti Gisborne District.

3.0 MANUAL FAULT-MAPPING METHODOLOGY

3.1 Data Sources

A review was undertaken of existing sources of fault mapping and recurrence interval information in Tairāwhiti Gisborne District, including:

1. The high-resolution version of the New Zealand Active Faults Database (which in Tairāwhiti Gisborne District is largely from 1:50,000-scale field and compilation mapping used by Mazengarb et al. [1991] and Mazengarb and Speden [2000]).
2. The 1:250,000-scale version of the New Zealand Active Faults Database (Langridge et al. 2016) (which in Tairāwhiti Gisborne District is largely from QMAP Raukumara – Mazengarb and Speden [2000]).
3. Lower-resolution (~1:1,000,000-scale) compilations such as the 2010 National Seismic Hazard Model (Stirling et al. 2012) and the New Zealand Community Fault Model (Seebeck et al. 2022).
4. Published maps, reports and scientific journal papers, referenced in Section 4.
5. Unpublished GNS Science consultancy and science reports, referenced in Section 4.
6. The authors' first-hand knowledge of the geology and active faulting in the district.

The LiDAR data used in this study are 1 m digital elevation and hillshade models (illuminated from different directions) developed from the 4 pulses per m^2 dataset commissioned in 2018–2020 by Te Kaunihera o Te Tairāwhiti Gisborne District Council. Land Information New Zealand orthophoto mosaics were also consulted.

3.2 Mapping and Attributing Active Fault Traces

An active fault is commonly made up of multiple fault features, which we refer to as traces.[3] Traces have been mapped using the LiDAR data in Tairāwhiti Gisborne District and are most commonly evident as fault scarps (steps), which range from relatively sharp to more rounded. A major challenge in the hill country of the district is distinguishing fault scarps from landslide scarps (head or side scarps). The distinction is ultimately a judgement based on the authors' mapping experience, but criteria include fault traces that: (1) are generally straighter than landslide head scarps; (2) cut across hilltops, landslides, or terraces; and/or (3) follow faults separating geological units (bedrock faults). Where it is geologically reasonable that traces may continue across landslides or streams, and they have been either eroded or buried linking traces have been inferred using a straight line or reasonable curve.

The accuracy with which the location of an active fault trace can be captured in a database is influenced by two types of uncertainty. The first is the uncertainty associated with how accurately the feature can be located on the ground. The second is the uncertainty associated with capturing that position into the database.

The locational accuracy of the fault on the ground is defined by the Accuracy and Surface Form attributes (Tables 3.1 and 3.2). In Tairāwhiti Gisborne District, many of the fault traces are very sharp or distinct in the LiDAR data and so have been attributed as accurate (Accuracy)

3 'Trace' is the basic mapping unit in the New Zealand Active Faults Database (Jongens and Dellow 2003; Langridge et al. 2016) and is a line of any length that is the intersection of a fault plane with the ground surface (see Appendix 1). Traces can be visible or concealed, and 'trace' and 'fault' are sometimes used interchangeably throughout this report.

and well expressed (Surface Form). Traces that are less clear because they are likely older ruptures or where the LiDAR resolution is lower (e.g. in the dense forested areas in the north and west) are generally attributed as approximate (Accuracy) and/or moderately expressed (Surface Form). Traces that have been inferred across landslides or rivers have been assigned either 'concealed' or 'inferred' (Accuracy) and 'not expressed' (Surface Form), respectively. For faults for which FAZs have been defined, the width of the fault feature is also captured in the Deformation Width attribute (Table 3.1), which is used in the construction of FAZs as described in Section 3.3.

The uncertainty associated with capturing the position of a fault trace in the database refers to the uncertainties introduced in the transfer of the fault location to a map. In this study, all faults were mapped in a GIS using LiDAR data, so this uncertainty (Capture Uncertainty) is considered to be relatively small (±3 m) and consistent for all of the traces.

An additional uncertainty with regard to using topographic fault features to define the location of past, and future, surface rupture and hazard is that the preservation potential of fault traces typically varies according to size. That is, a large scarp or displacement is more likely to be preserved in the landscape than a small scarp or displacement. So, even when a distinct fault feature is identified at a site, it is possible that smaller, but still damaging (or life-threatening), displacements occurred elsewhere but evidence for those faults is no longer preserved in the landscape. Thus, an identified fault feature may not record the true scale of fault-rupture hazard at a site. As is discussed in more detail in Section 3.3, this type of uncertainty is typically addressed by prescribing a 20 m 'setback' distance either side of the mapped fault.

Another important uncertainty for the mapped traces is whether they are in fact active fault features or whether they could have formed by some other non-tectonic process, such as gravitational processes (i.e. landslides), as discussed earlier. In practise, this means that a narrow feature may be accurately mapped along a feature in the LiDAR data, but this does not necessarily mean it is an active fault. This uncertainty is captured in the Tectonic Origin attribute and is an expert assessment of confidence in whether the feature has formed as a result of ground-surface fault rupture or some other process.

The attributes assigned to each fault trace mapped in Tairāwhiti Gisborne District are listed in Table 3.1.

Table 3.1 Attributes for mapped active fault traces in Tairāwhiti Gisborne District used for the purposes of developing Fault Avoidance Zones and Fault Awareness Areas.

Attribute	Field Name in Shapefile	Definition
Fault Name	Fault_name	The name given to an active fault.
Accuracy	Accuracy	Accuracy of the location of the fault on the ground surface (accurate, approximate, concealed or inferred).
Dominant Slip Type	DOM_SLIPTY	Dominant or primary sense of movement on the fault (normal, reverse or strike-slip – see Appendix 1 for definitions).
Down-thrown Quadrant	DOWN_QUAD	The direction of the down-thrown side of the fault described in terms of compass quadrants.
Tectonic Origin	Tect_orig	Certainty that the feature is of tectonic (e.g. earthquake) origin (definite, likely or possible).

Attribute	Field Name in Shapefile	Definition
Surface Form	Surface_fo	How clearly the mapped feature can be seen on the ground (well expressed, moderately expressed, not expressed or unknown – see Table 3.2 for details).
Fault Complexity	Fault_comp	The width and distribution of the deformed land around the fault trace (well defined, well-defined extended, uncertain constrained – see Table 3.3 for further details).
Deformation Width of Local Fault Feature	Deform_wid	Horizontal width of the visible fault feature or, for concealed faults or faults with no surface trace, the maximum width of where the deformation could be located. Value is in metres.
Recurrence Interval Class	RI_class	The average time between surface-rupturing events on a fault, grouped into six classifications (RI Classes I–VI – see Table 3.4 for a full list and further details).

Table 3.2 Definitions of Surface Form categories, assigned to Fault Awareness Areas (from Barrell et al. [2015]).

Category	Definition
Well expressed	The mapped feature should be able to be located on the ground to better than ±50 m – it can be clearly seen on the ground.
Moderately expressed	The mapped feature should be able to be located on the ground to better than ±100 m – it is not so easily seen on the ground.
Not expressed	The mapped feature cannot be seen at the ground surface and would require detailed investigation to locate it (for example, it has been covered by river gravels since the last movement on the fault).
Unknown	This term is applied where, for example, vegetation obscures the ground surface; where the natural landscape has been heavily modified by humans and the degree of expression cannot be assessed using aerial or satellite photos; or where no photos of suitable scale, or other data such as LiDAR, are available for making an assessment.

Table 3.3 Definitions of fault complexity terms used to develop Fault Avoidance Zones. Adapted from the MfE Active Fault Guidelines (Kerr et al. 2003).

Fault Complexity	Definition
Well defined	Fault rupture deformation is well defined and of limited geographic width (e.g. metres to tens of metres wide).
Well-defined extended	Fault rupture deformation has been either buried or eroded over short distances, but its position is tightly constrained by the presence of nearby distinct fault features.
Distributed	Fault rupture deformation is distributed over a relatively broad, but defined, geographic width (e.g. tens to hundreds of metres wide), typically as multiple fault traces and/or folds.
Uncertain constrained	Areas where the location of fault rupture is uncertain because evidence has been either buried or eroded, but where the location of fault rupture can be constrained to a reasonable geographic extent (≤300 m).
Uncertain poorly constrained	The location of fault-rupture deformation is uncertain and cannot be constrained to lie within a zone less than 300 m wide, usually because evidence of deformation has been either buried or eroded away, or the features used to define the fault's location are widely spaced and/or very broad in nature.

Table 3.4 Definition of Recurrence Interval (RI) classes from the MfE Active Fault Guidelines (Kerr et al. 2003). In practise, only two faults in Tairāwhiti Gisborne District were assigned to a RI Class, and these are RI Class II or III. See Section 3.5 for more discussion regarding recurrence interval and Section 4.3.1 for detail regarding RI Class definition for the faults with FAZs in this report.

RI Class	Average Recurrence Interval of Surface Rupture
I	≤2000 years
II	>2000 to ≤3500 years
III	>3500 to ≤5000 years
IV	>5000 to ≤10,000 years
V	>10,000 to ≤20,000 years
VI	>20,000 to ≤125,000 years

3.3 Development of Fault Avoidance Zones

As is suggested in the MfE Active Fault Guidelines (Kerr et al. 2003), a FAZ is created by defining a 'Likely Fault Rupture Zone', buffered by an additional 20 m 'Setback Zone'. This additional 20 m is meant to encompass the intense deformation and secondary ruptures that can occur close to primary fault ruptures.

In this study, the 'Likely Fault Rupture Zone' is defined by buffering the traces by the Deformation Width (Figure 3.1a). The 'Likely Fault Rupture Zone' is then buffered by 3 m either side to account for the uncertainty in capturing the fault in the database (Capture Uncertainty), which is in turn buffered by 20 m each side to define the 'Setback Zone' (Figure 3.1a). The combined area under the various buffers is then termed the FAZ (Figure 3.1b).

Surface-rupture Fault Complexity is an important parameter used in the MfE Active Fault Guidelines to define rupture hazard at a site. The rationale is that, when fault-rupture deformation is distributed over a wide area, the amount of deformation at a specific locality within the distributed zone is lower than where the deformation is concentrated on a single well-defined trace. The relative fault-rupture hazard/risk is therefore less within a zone of distributed deformation than within a narrow, well-defined zone. Table 3.3 lists the Fault Complexity terms and definitions from the MfE Active Fault Guidelines. In practise, the two faults for which FAZs were constructed in this study are relatively simple, so only the well defined, well-defined extended and uncertain constrained terms were used.

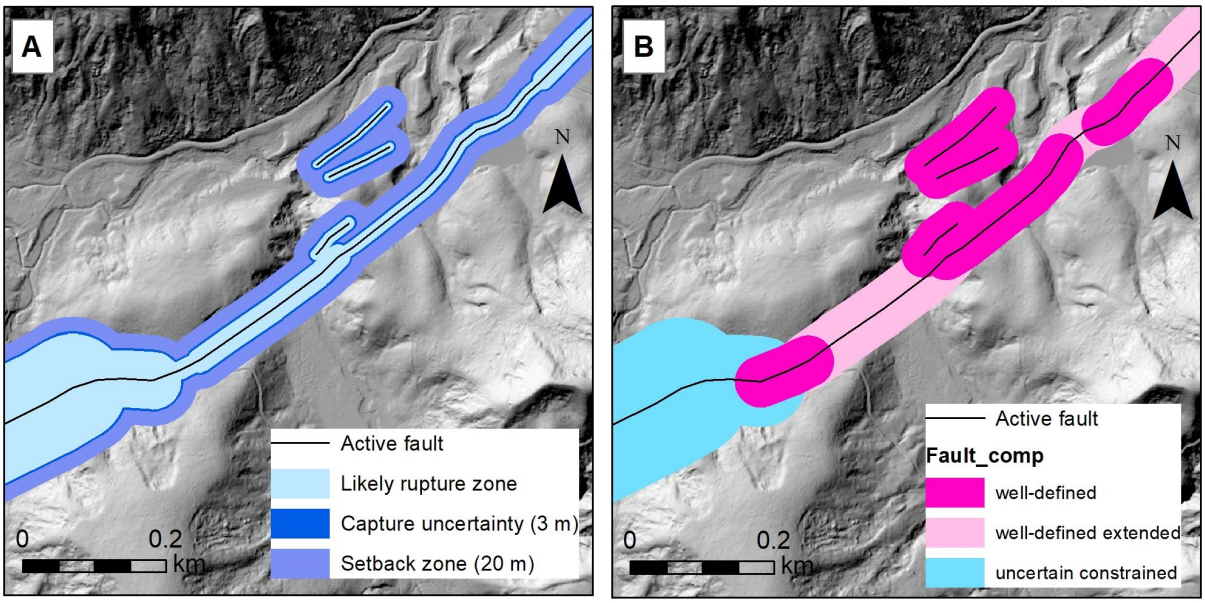

Figure 3.1 (a) The individual components (buffer zones) used to construct Fault Avoidance Zones. These are then combined to create the Fault Avoidance Zones. (b) The example is part of the Repongaere Fault, shown colour-coded by fault complexity (Fault_comp).

These Fault Complexity terms link directly into Resource Consent Category tables for the MfE Active Fault Guidelines (Appendices 2 and 3). These are also the same definitions used in similar active-fault-mapping projects in the Hawke's Bay region and elsewhere throughout the country (e.g. Van Dissen and Heron 2003; Van Dissen et al. 2005; Langridge and Ries 2014, 2016; Litchfield and Van Dissen 2014; Clark and Ries 2016; Langridge and Morgenstern 2019, 2020a, 2020b; Litchfield et al. 2019, 2020b, 2022; Langridge et al. 2021).

3.4 Development of Fault Awareness Areas

FAAs were developed in this study by defining a buffer of 125 m either side of the mapped fault. This follows the methodology used for faults mapped using LiDAR data or a detailed Digital Surface Model (DSM) in, for example, the Taupō District (Litchfield et al. 2020b), the Tararua District (Langridge et al. 2021) and the combined Wairarapa Districts (Litchfield et al. 2022). It differs from that of Barrell et al. (2015) in the Canterbury region, who were using faults mapped at 1:250,000 scale. That is, we consider a 250-m-wide buffer to appropriately encompass the uncertainty of faults mapped using LiDAR data to be overly conservatively wide and have thus adopted use of a narrower buffer.

Key attributes for FAAs are Tectonic Origin and Surface Form; both terms are defined in Table 3.1. Surface Form is further defined in Table 3.2 and plays a similar role to Fault Complexity for FAZs. The Environment Canterbury (ECan) FAA Guidelines by Barrell et al. (2015) recommended actions based on RI Class (see next section). Recurrence interval was not able to be defined for faults with FAAs in Tairāwhiti Gisborne District, but we include the ECan recommended actions in Appendix 3 (Table A3.3) as a point of reference should recurrence intervals be able to be defined in the future.

3.5 Recurrence Interval Classes

The average recurrence interval of ground-surface fault rupture is the average number of years between successive ground-surface-rupturing earthquakes along a specific section or length of fault. Typically, the longer the average recurrence interval of surface rupture on a fault, the less likely the fault is to rupture in the near future. Likelihood of rupture is also a function of other variables, such as elapsed time since the last rupture of the fault and the size, style and timing of large earthquakes on other nearby faults; however, these variables are not used to define rupture hazard in the MfE Active Fault Guidelines. Broadly speaking, a fault with a long recurrence interval typically poses less of a hazard than one with a short recurrence interval. In the MfE Active Fault Guidelines and the recommended actions for FAAs (Barrell et al. 2015), active faults are grouped according to RI Class (Table 3.4), such that the most hazardous faults, i.e. those with the shortest recurrence intervals, are grouped within RI Class I. The next most active group of faults are those within RI Class II, and so on.

Paleoseismic trenching investigations have only been undertaken for one fault in Tairāwhiti Gisborne District (the Repongaere Fault; Berryman et al. 2009), so the recurrence interval for most faults is unknown. It is also challenging to estimate recurrence interval for faults in the hill country because of a lack of suitable faulted features of known age. Most faults have therefore not been assigned to a RI Class in this study.

4.0 MANUAL FAULT-MAPPING RESULTS

4.1 Summary of Tairāwhiti Gisborne District Active Faults

As anticipated, the use of LiDAR data to map active faults in Tairāwhiti Gisborne District has resulted in the identification of many more traces than in previous studies (compare Figures 4.1 and 1.2). Short traces have been mapped in a number of places throughout the district, and the most continuous newly identified faults are concentrated in the west and south. Of these, the longest fault mapped, at ~11 km, is still relatively short compared with faults in other parts of Aotearoa New Zealand (e.g. Figure 1.1).

Such short lengths supports previous interpretations that these faults are likely secondary rather than primary faults. That is, these faults are unlikely to extend down to seismogenic depths (10–15 km) and/or the Hikurangi Subduction Zone (interface) and rupture on their own in M6.5+ earthquakes. Instead, they are likely to be faults that may rupture: (1) on their own in smaller earthquakes to accommodate rapid uplift driven by subduction processes at depth, or (2) with earthquakes on other faults (e.g. the North Island Dextral Fault Belt to the west or offshore faults to the east) or (3) on the Hikurangi Subduction Zone (interface). While all of the mapped faults pose a surface-rupture hazard, the main implication for planning purposes is for characterising recurrence interval, as secondary faults may not have a regular recurrence interval that can be readily defined.

Newly identified faults have been assigned preliminary names from nearby geographic features and are distinguished by a lower case ‘f’ – e.g. Pukeopou fault. In general, faults are only assigned names when they are several (>3) km in length, but a few shorter faults have previously been named and these have been retained for historical consistency. A few previously mapped faults, such as the Motu Fault, do not have visible active fault traces in the LiDAR data and so have now been removed from the active fault dataset.

The sense of movement is not easy to define for most active faults identified in Tairāwhiti Gisborne District because of a lack of suitable geomorphic features. Most have therefore been classified as normal faults based on a few known exposures and previous interpretations (Mazengarb 1984; Thornley 1996; Berryman et al. 2009), but a handful have tentatively been inferred to be strike-slip or reverse based on the shape of their traces across topography. For example, straight traces cutting across hilly topography are likely to be steeply dipping and therefore strike-slip faults.

RI Classes have only been assigned to two faults and are summarised in Table 4.1 and discussed in Section 4.3.1.

Table 4.1 Recurrence Interval (RI) Class information for active faults in Tairāwhiti Gisborne District.

Fault	RI Class	RI Class (Years)	RI Class Confidence*	Data Sources
Repongaere	III	>3500 to ≤5000	M	Berryman et al. (2009)
Pakarae	II	>2000 to ≤3500	M	Ota et al. (1991); Wilson et al. (2006); Litchfield et al. (2020a)

* **Notes:** RI Class Confidence: M, Medium – uncertainty in average recurrence interval encompasses a significant proportion (>~25%) of two RI Classes, and the mean of the uncertainty range typically determines into which class the fault is placed.

The active fault mapping for Tairāwhiti Gisborne District in this study is discussed in the following sections, starting with those in and around the priority 1 areas (Section 4.2), followed by previously mapped faults (Section 4.3; priority 2), newly identified active faults (Section 4.4) and, finally, faults near critical infrastructure (priority 2) and remaining faults (priority 3; Section 4.5).

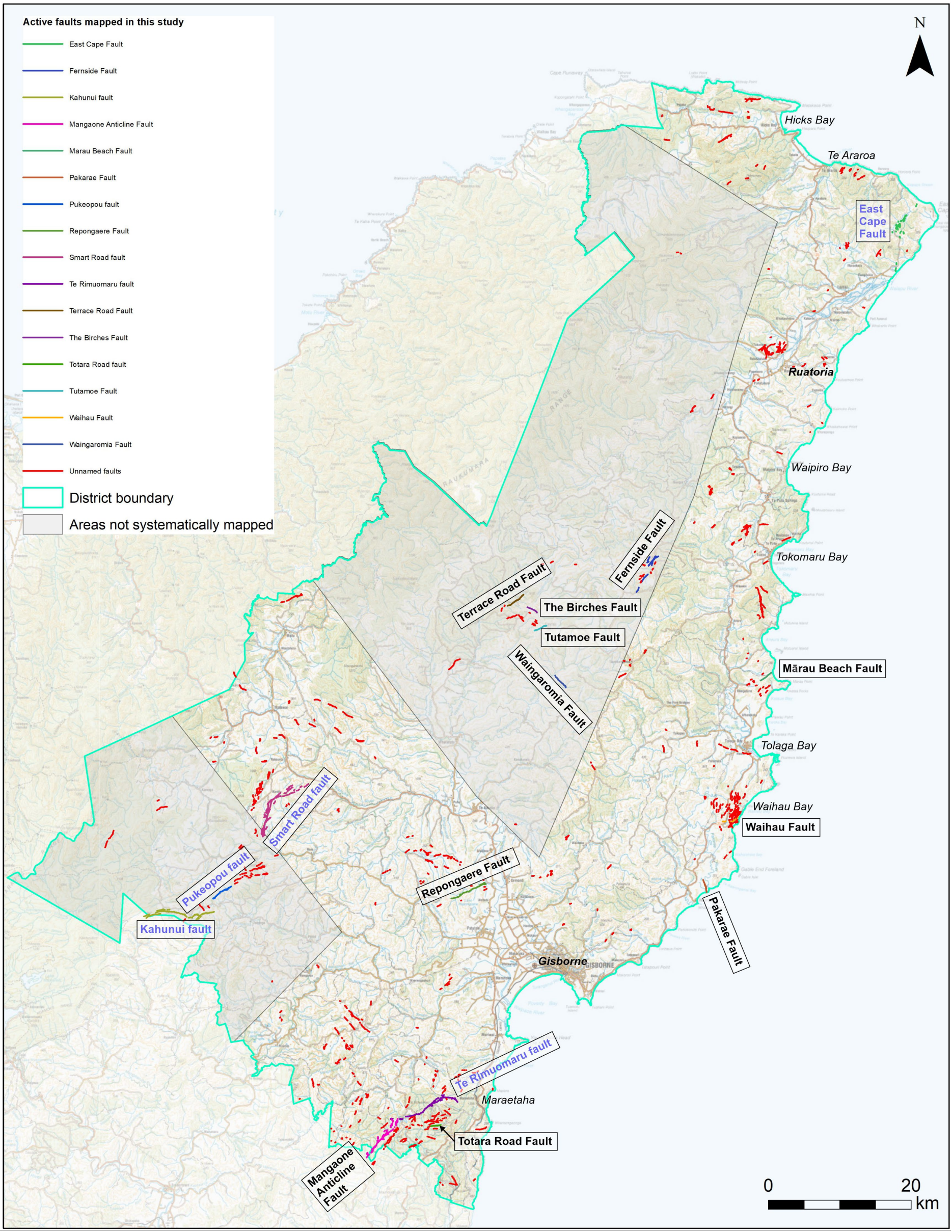

Figure 4.1 Active faults in Tairāwhiti Gisborne District mapped in this study. Named faults are coloured, unnamed faults are red and newly identified active faults are labelled in blue.

This page left intentionally blank.

4.2 Priority 1 Areas – Towns

None of the priority 1 areas around the main towns were crossed by, or included, previously mapped active faults (Figure 1.2), and the new mapping in this study did not identify any new traces in the **Gisborne** or **Te Araroa** priority 1 areas. However, short active fault traces were identified in the Tolaga Bay, Tokomaru Bay and Ruatoria priority 1 areas. These traces all have a Tectonic Origin of 'possible' and are short (≤4.7 km), so they have not been named (because they may actually not be fault traces). Nevertheless, FAAs have been developed for them to highlight the potential hazard they pose should they actually be faults.

A set of discontinuous traces have been mapped crossing the south part of **Tolaga Bay** town (and State Highway 35) and extending 3.5 km to the west (Figure 4.2). The traces are subtle in the LiDAR data, but cross beach ridges in the town area and are oriented at a high angle to Waimaunu Stream, therefore these are considered unlikely to be beach or fluvial features. The scarp crossing the beach ridges is lower in the east than the west, which suggeststhat, if it is an active fault, it is possible that there were two or more ground-surface-rupturing earthquakes since the beach ridges were formed, likely within the last 7500 years when sea level reached approximately the current level (Clement et al. 2016). This would suggest a maximum recurrence interval of 3750–7500 years. We strongly recommend further investigations of the traces and/or the ages of the beach ridges and fluvial terraces, such as ground-penetrating radar (GPR), age sampling (e.g. radiocarbon, volcanic ash [tephra]) and/or paleoseismic trenching to help confirm whether they are fault traces.

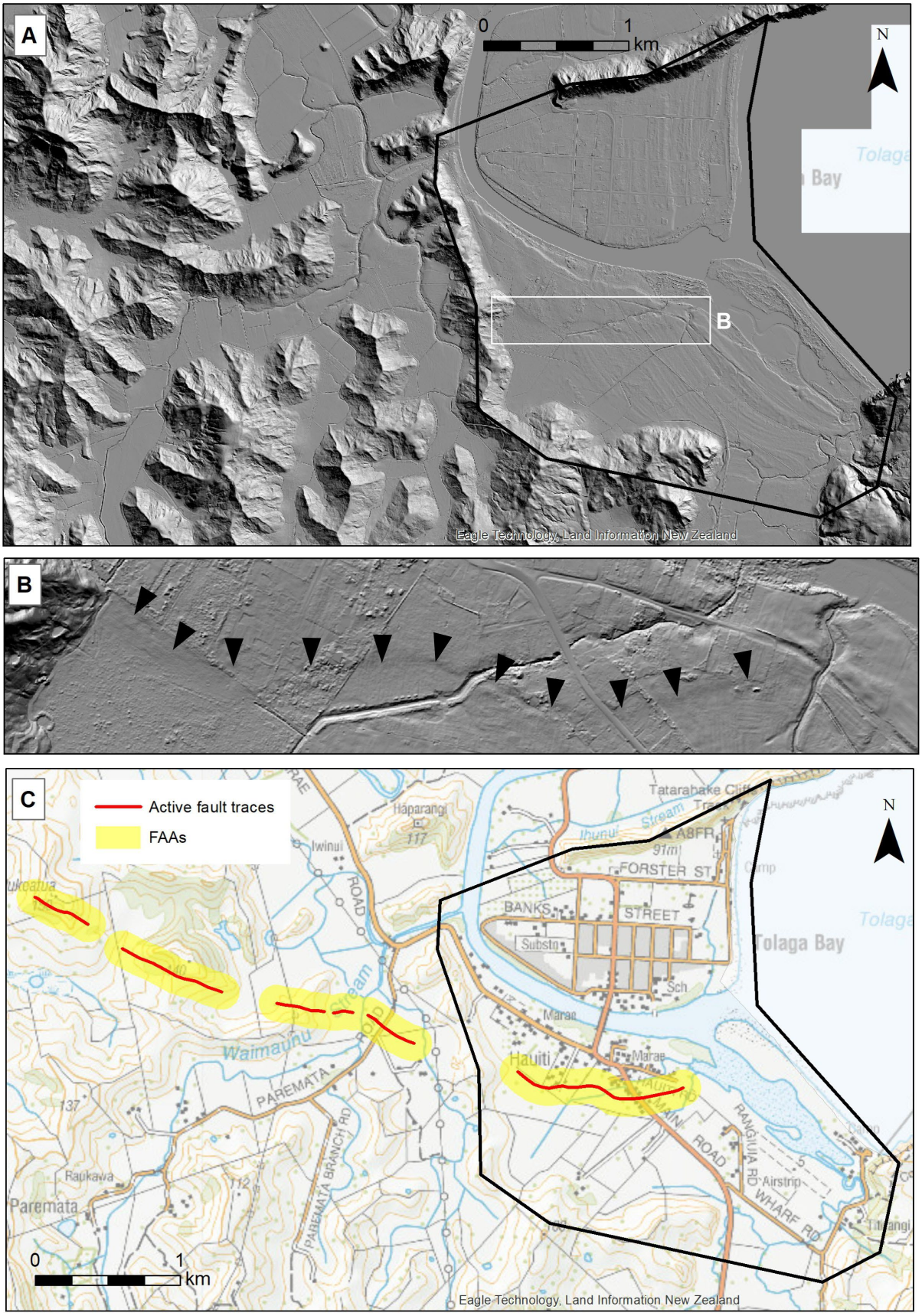

Figure 4.2 Tolaga Bay priority area (black outline). (a) LiDAR hillshade map (illuminated from the northeast). (b) Enlargement of the fault trace crossing southern Tolaga Bay town and State Highway 35. LiDAR hillshade map (illuminated from the northwest). (c) Active fault traces and FAAs.

Two short (≤1.2 km) traces have been mapped in the hills above **Tokomaru Bay** (Figure 4.3). The northern feature is a series of eroded scarps and linear ridges and does not appear to extend across Waitakeo Stream to the south. The southern feature crosses a hilltop and separates smooth ground to the north from more hummocky ground to the south and is likely to have been re-activated in part as a landslide. Further investigations could potentially be undertaken on these features to confirm their tectonic origin, such as GPR, age sampling and/or paleoseismic trenching.

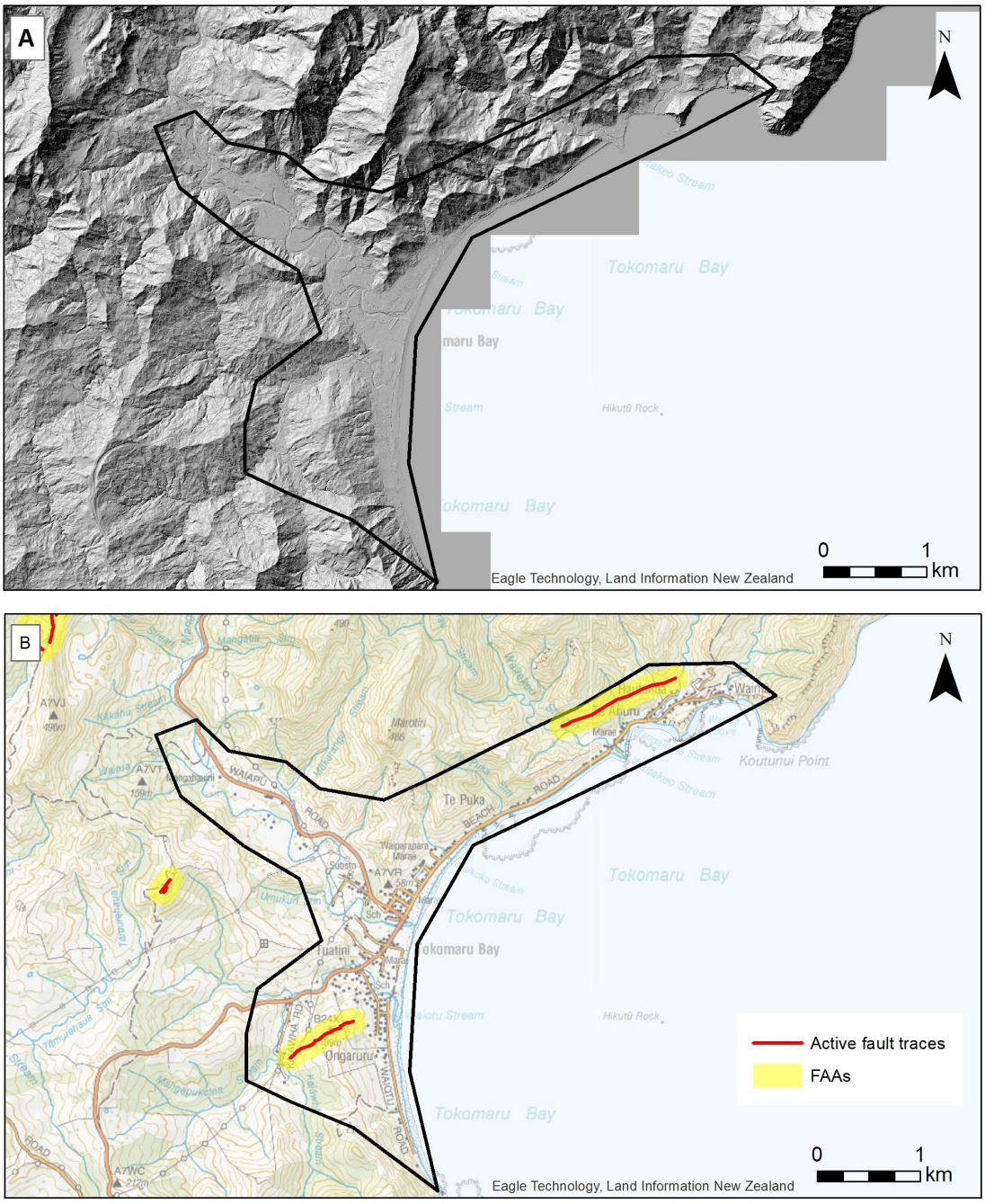

Figure 4.3 Tokomaru Bay priority area (black outline). (a) LiDAR hillshade map (illuminated from the northwest). (b) Active fault traces and FAAs.

Two short (≤700 m) traces have been mapped in the eastern part of the **Ruatoria** priority 1 area, east of the town (Figure 4.4). The western trace is a straight, clear step in the alluvial fans coming off the hills to the south. It is sub-parallel to Tuparoa Road and a drainage ditch, so it is possible that it is a man-made feature. The eastern traces are more subtle steps across

the fans on either side of, and at high angle to, Mangaraeia Stream. The orientation of these features at a high angle to the stream means it is unlikely that they were formed by the stream. Both features are worthy of further investigation to confirm their tectonic origin, including community consultation (on the possibility of the traces being man-made in origin) and using GPR, age sampling and/or paleoseismic trenching.

Newly identified traces have also been mapped west and north of the **Ruatoria** priority 1 area (Figure 4.4). Several of those to the north, mainly on the high fluvial terraces above the Waiapu River, have a Tectonic Origin classification of 'likely'. All are short but are also worthy of further investigation to investigate their tectonic origin.

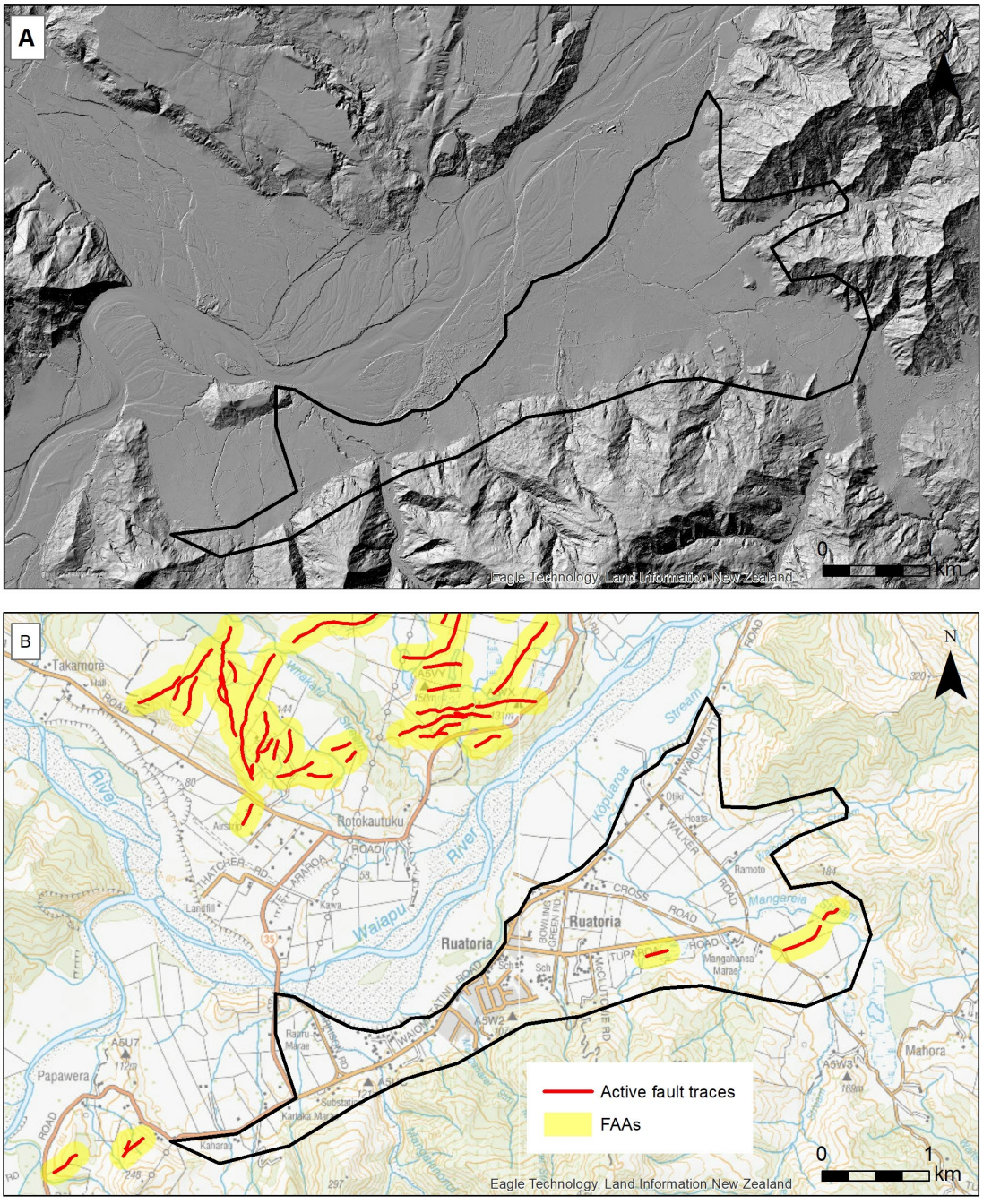

Figure 4.4 Ruatoria priority area (black outline) (A) LiDAR hillshade map (illuminated from the northwest). (B) Active fault traces and FAAs.

4.3 Previously Mapped Faults (Priority 2)

In this section, we describe the new mapping of previously mapped, named faults. We first describe the two faults for which we have developed FAZs, then the remainder (with FAAs) broadly from north to south, followed by faults that do not have visible traces in the LiDAR data and so have been removed from the active fault dataset. The named faults are shown in different colours on Figure 4.1, and close-up maps of the individual faults are included below (note that the scales for each map differ).

4.3.1 Previously Mapped Faults now with Fault Avoidance Zones Defined

The **Repongaere Fault**, ~15 km inland of Gisborne (Figure 4.1), is currently the only fault in Tairāwhiti Gisborne District to have been investigated through paleoseismic trenching (Berryman et al. 2009) (Figure 4.5). Three trenches were excavated at two sites near either ends of the well-defined traces, but a fault plane was not found in one of the trenches. In the other two trenches, a normal fault, dipping to the southeast, cut volcanic ash (tephra) layers, indicating that the last fault rupture was ~3400 years ago with a previous one ~13,800–5470 years ago. From this, a slip rate of ~0.1 mm/yr and a maximum recurrence interval of 4500–6900 years was obtained. This straddles RI Classes III (>3500 to ≤5000 years) and IV (>5000 to ≤10,000 years) (Table 3.4), but, as it is a maximum, we conservatively place it in RI Class III with medium confidence (Table 4.1).

Figure 4.5 Exposures of the Repongaere Fault in a paleoseismic trench (trench 1 of Berryman et al. [2009]; located on Figure 4.6). Two fault planes, marked by the yellow arrows, were exposed in the trench. The southern-most of the two fault planes projects upwards to the base of the fault scarp (step in the ground surface).

The mapping of the Repongaere Fault in this study (Figure 4.6) is broadly similar to that of Berryman et al. (2009), with clear, sharp traces assigned a Fault Complexity of well-defined at the east end and along Pouaru Stream (maximum width 66 m). Additional, sub-parallel, traces have also been mapped north of the main traces in these two areas. In between the well-defined traces, and farther west, traces have been inferred and a Fault Complexity of uncertain constrained assigned, with wider FAZs (≤196 m), to reflect the greater locational uncertainty.

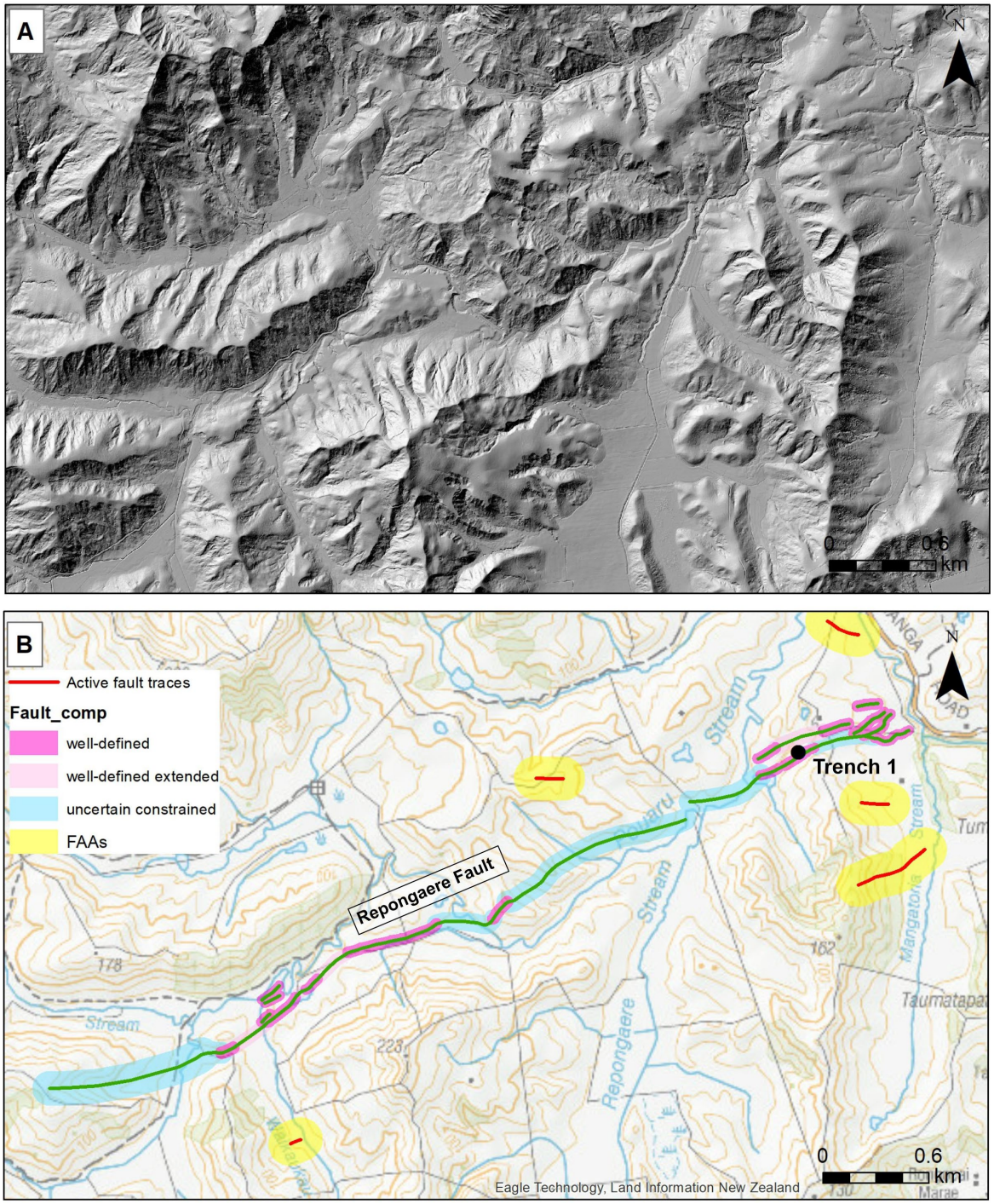

Figure 4.6 The Repongaere Fault (green) and other nearby possible fault traces (red). (a) LiDAR hillshade map (illuminated from the northwest). (b) Active fault traces, FAZs (Repongaere Fault only; coloured by Fault Complexity – Fault_comp) and FAAs on other fault traces. The black dot denotes the location of trench 1 of Berryman et al. (2009), shown in Figure 4.5.

The **Pakarae Fault**, at the Pakarae River mouth (Figure 4.1), has also received some investigation during studies of earthquake uplift of the Holocene (post-7500 years) marine terraces that are displaced by the Pakarae Fault (Ota et al. 1991; Wilson et al. 2006; Litchfield et al. 2020a). An offshore continuation of the Pakarae Fault has recently been mapped (Litchfield et al. 2020a), but it has always been a challenge to map active traces along the bedrock fault inland of the coast. In this study, three sub-parallel traces have been mapped extending ~1.8 km inland (Figure 4.7), but there is no visible expression of the Pakarae Fault in the LiDAR data in the surrounding hills or within the Pakarae River valley. The height of the Pakarae Fault scarp decreases seawards, indicating that two or more earthquakes have

displaced the progressively younger marine terraces. The marine terraces cannot be matched across the fault because some are buried by sand dunes on the western side of the fault, therefore earthquake ages cannot be inferred. Wilson et al. (2006) showed that the Pakarae Fault did not rupture with every earthquake that uplifted the marine terraces east of the fault. Together, the available data suggests that the recurrence interval is likely between 850 and 3750 years, so we place it in RI Class II (>2000 to ≤3500 years) with moderate confidence (Table 4.1). A FAZ with a Fault Complexity of 'well defined' has been developed for the clearest trace. Extensions of the Pakarae Fault to the north and south have been mapped, and these have been assigned Fault Complexities of uncertain constrained and well-defined extended, respectively (Figure 4.7). All FAZs are relatively narrow (≤126 m wide).

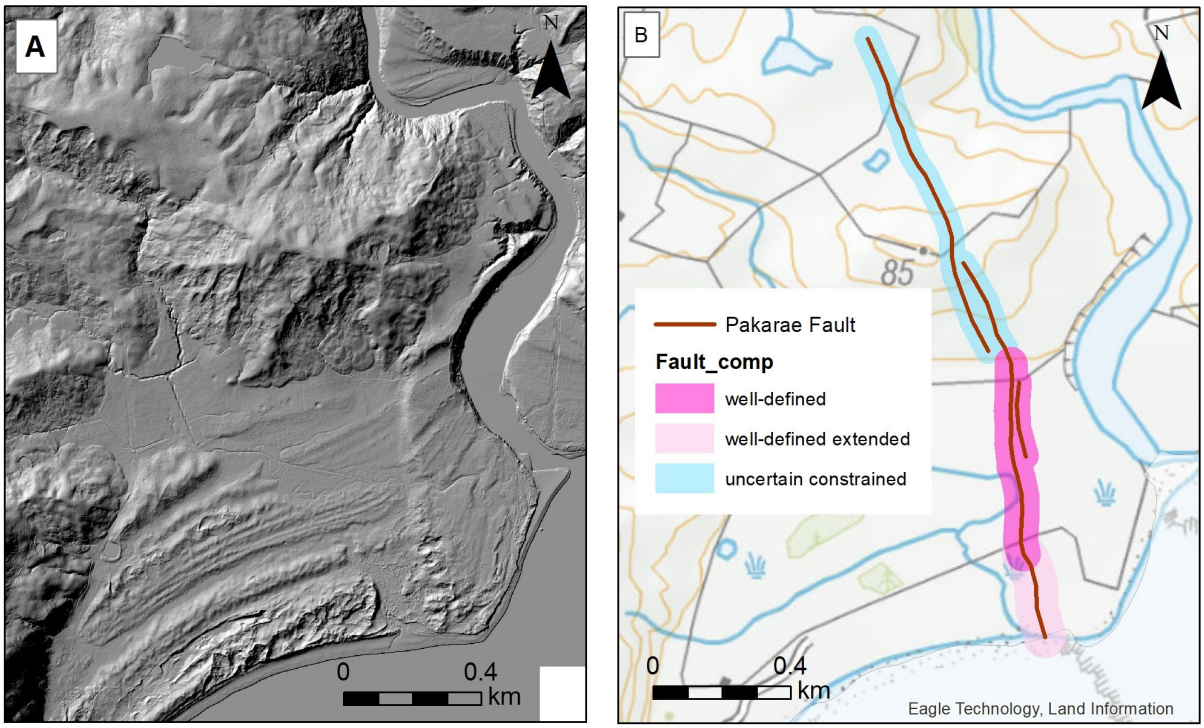

Figure 4.7 The Pakarae Fault at Pakarae River mouth. (a) LiDAR hillshade map (illuminated from the northwest). (b) Active fault traces and FAZs coloured by Fault Complexity (Fault_comp).

4.3.2 Previously Mapped Faults now with Fault Awareness Areas Defined

The **Fernside Fault**, located ~16 km inland of Tokomaru Bay, is another fault that has had some previous study (Mazengarb 1984; Thornley 1996) but no paleoseismic investigations. The Fernside Fault is a relatively long (~23 km) normal bedrock fault (Mazengarb and Speden 2000), but the mapping in this study only identified active fault traces along ~2 km of the central part of the previously mapped fault (Figure 4.8) and some possible traces to the south (Figure 4.1). In the central ~2 km, there are multiple clear, sharp traces, some branching off each other and some sub-parallel to the bedrock fault. Two sets of traces northwest of the main fault are very straight and so have tentatively been classified as strike-slip faults. The name 'Fernside Fault' has been retained for traces along or close to the bedrock fault, but it is possible that the other unnamed traces nearby could rupture in an earthquake on the Fernside Fault.

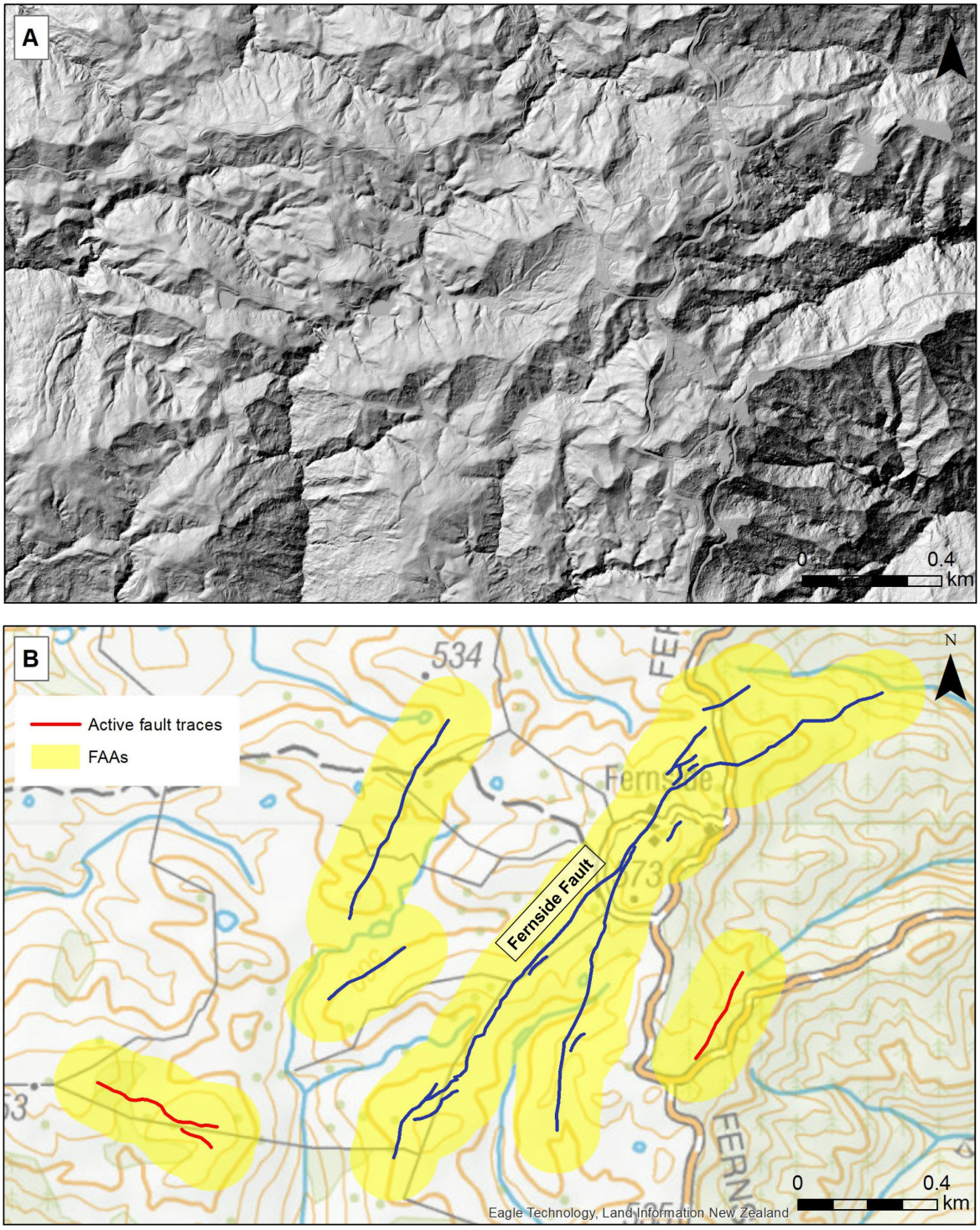

Figure 4.8 The northern part of the Fernside Fault (blue) and nearby possible fault traces (red). (a) LiDAR hillshade map (illuminated from the northwest). (b) Active fault traces and FAAs.

Four, isolated, active faults were mapped by Mazengarb et al. (1991) west of Tauwhareparae (Figure 4.1, Figure 4.9). These were previously informally named the **Terrace Road Fault**, **Tutamoe Fault**, **The Birches Fault** and **Waingaromia Fault**. The mapping in this study has confirmed the existence of all of these fault traces and extended their lengths to a maximum of 2.2 km (Waingaromia Fault). The traces are clearest on The Birches and Waingaromia faults. A number of other traces of similar orientations have also been mapped nearby. The short lengths of each of these faults means that it is questionable whether these are significant, primary active faults that should have official names ascribed to them, but the informal names previously give to them by Mazengarb et al. (1991) are retained here for historical consistency.

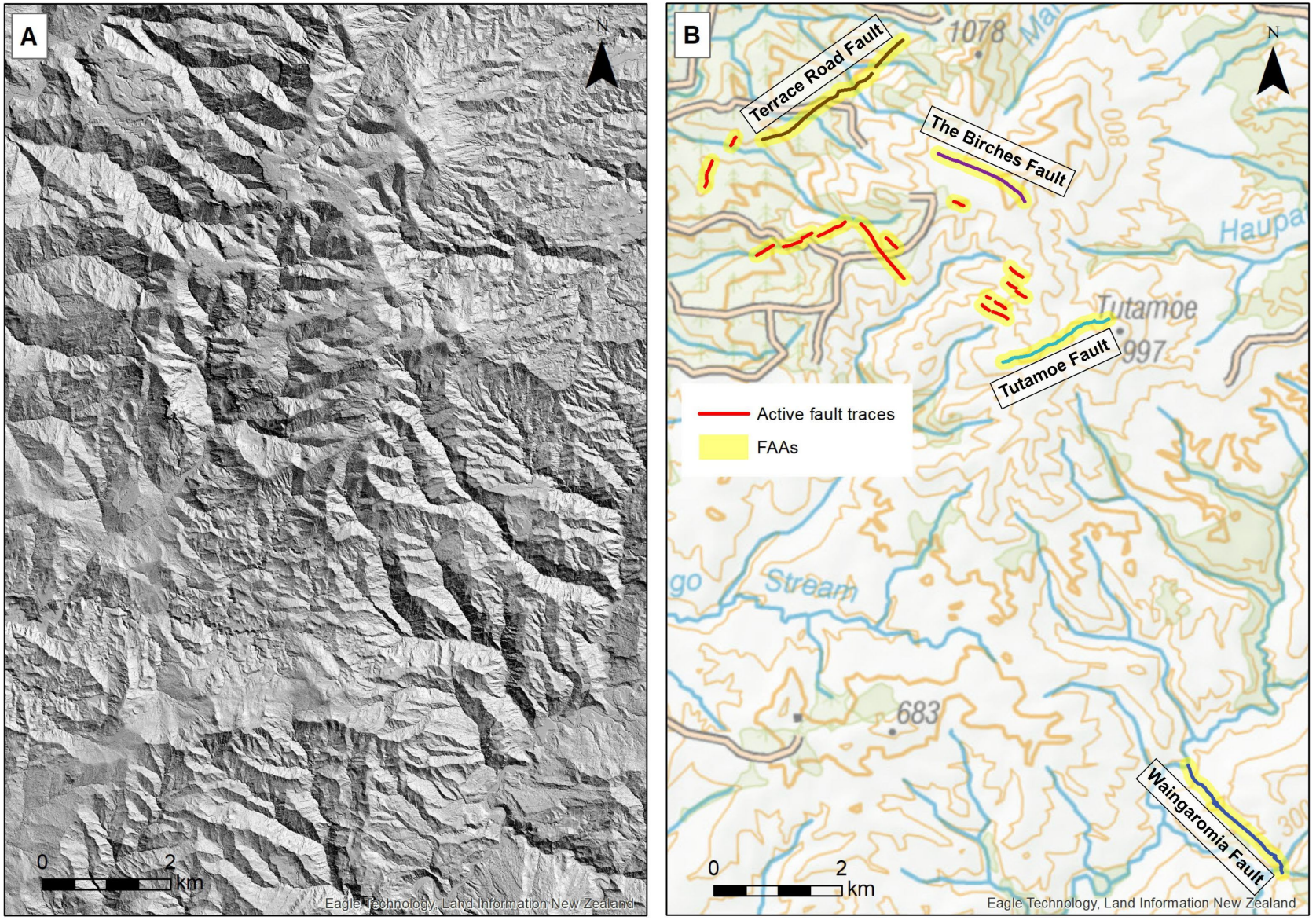

Figure 4.9 Faults west of Tauwhareparae. (a) LiDAR hillshade map (illuminated from the northeast). (b) Active fault traces and FAAs.

The **Mārau Beach Fault**, at Mārau Beach, ~10 km north of Tolaga Bay (Figure 4.1), was previously mapped from aerial photographs and visited in the field by Francis (1983). The mapped trace in this study (Figure 4.10) is slightly shorter than the previously mapped version, although there are some unnamed traces further southwest that could be a continuation of the Mārau Beach Fault, and coastal landsliding means that it is ambiguous whether it continues northeast to the coast (and hence offshore) or not. The overall trace is relatively straight, but the shape as it climbs southwest out of Raponga Stream valley may suggest that it is a northwest-dipping reverse fault rather than a normal fault. The overall length is ~1.9 km, but, because it possibly continues offshore and for historical consistency, the name is retained.

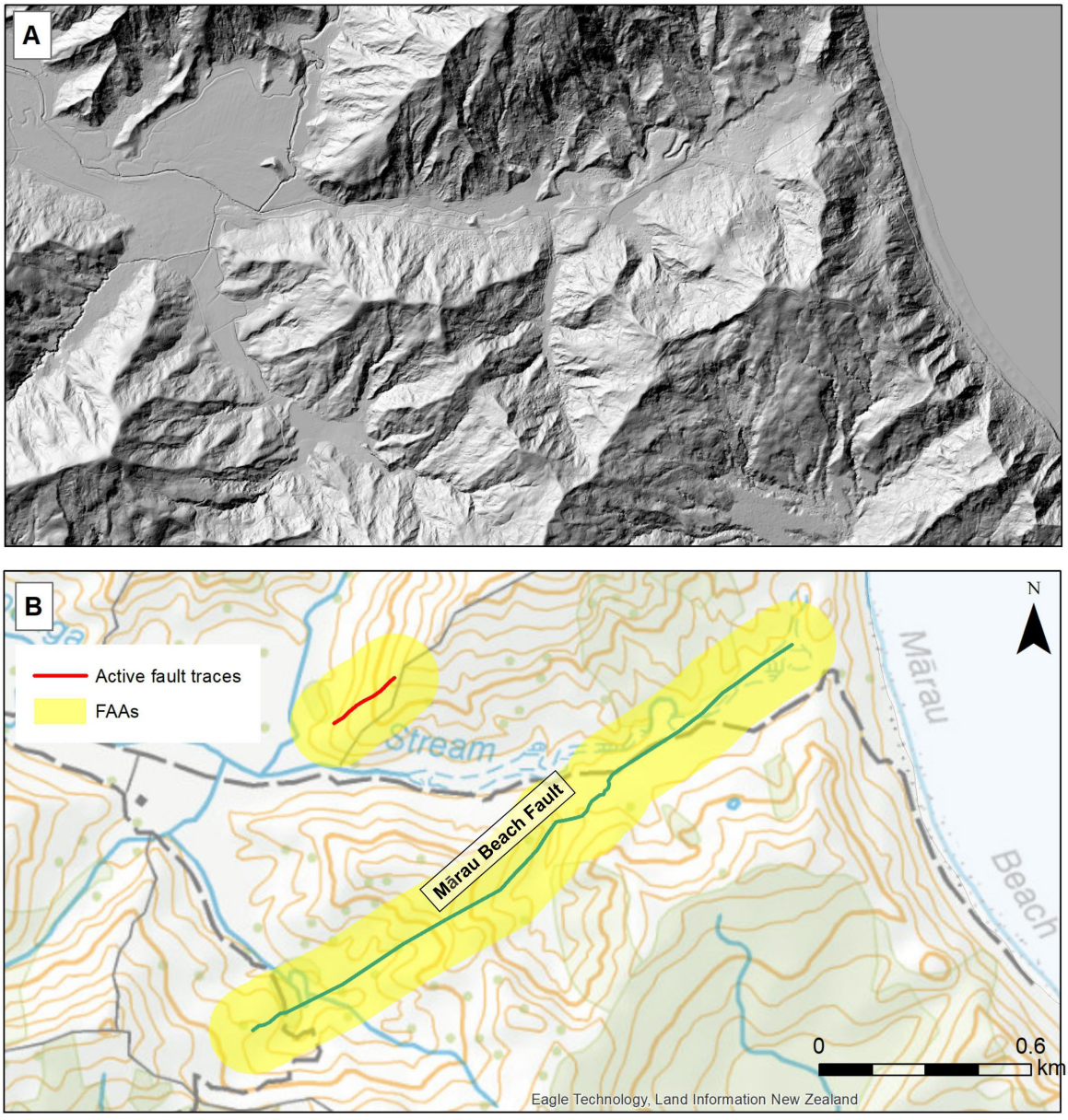

Figure 4.10 The Mārau Beach Fault (green) and nearby possible fault trace (red). (a) LiDAR hillshade map (illuminated from the northwest). (b) Active fault traces and FAAs.

Active fault traces in the vicinity of Waihau Beach – Loisels, and in particular a prominent scarp damming drainage and crossing Waihau Road, have long been known about (K Berryman, pers.comm.) and informally referred to as the **Waihau Fault** (e.g. Litchfield et al. 2020a). In this study, the southwest-trending trace has been confirmed and extended southwest for a total length of ~1.3 km (Figure 4.11). The northeast end of the fault is affected by coastal landsliding, so it is ambiguous whether it continues to the coast and hence offshore. The north-

trending previously mapped traces are interpreted to be landslide scarps, but a broad set of possible traces have been mapped north and south, particularly on the plateau to the north. The distribution of this broader set of traces is enigmatic and may suggest secondary faulting related to the Waihau Fault, or a feature associated with the Hikurangi Subduction Zone at depth or possibly offshore. Like the Mārau Beach Fault, the name is retained due to the possibility that it continues offshore and for historical consistency.

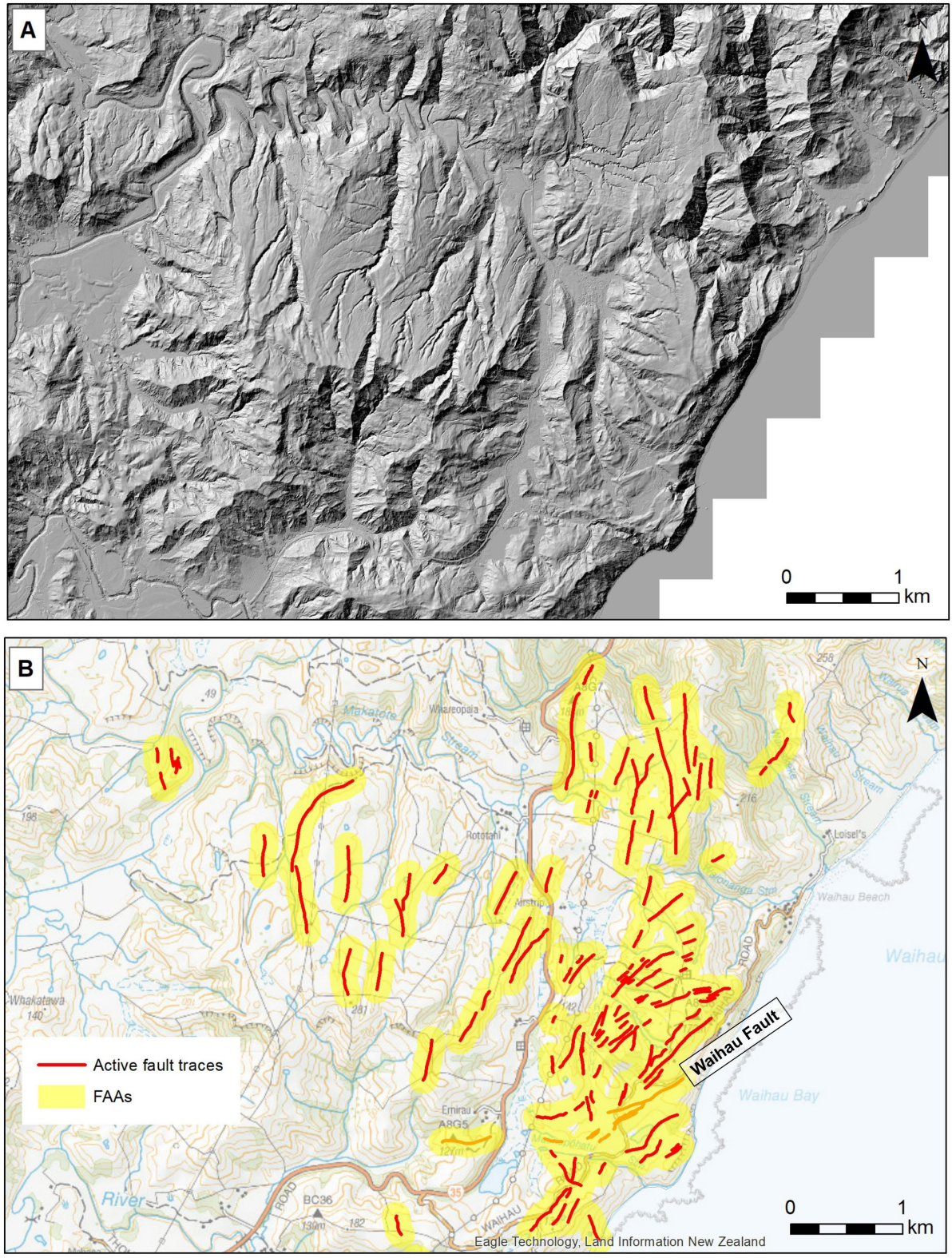

Figure 4.11 The Waihau Fault (orange) and nearby fault traces (red). (a) LiDAR hillshade map (illuminated from the northwest). (b) Active fault traces and FAAs.

A series of active faults were previously mapped from aerial photographs in the hills southwest of Maraetaha by Francis (1984) (Figure 1.2), and some of the longest faults were included in QMAP Raukumara (Mazengarb and Speden 2000). One of these, informally referred to as the **Totara Road Fault**, was confirmed in the field by Francis (1984) and is very clear in the LiDAR data, with a straight trace (Figure 4.12) that is tentatively inferred to have strike-slip sense of movement. The total length is ~1.5 km, but we retain the name because it is such a prominent trace and for historical consistency. Traces have been mapped along several of the previously mapped faults, along with a number of other newly identified, short (≤1.1-km-long) traces (Figure 4.12). Two sets of traces are continuous enough that they have been assigned names. The first is the 10-km-long **Te Rimuomaru fault**, which extends from west of the water supply reservoirs, crosses Te Rimuomaru hill and ends ~600 m east of the eastern edge of Waterworks Bush. Many of the traces are relatively sharp, which may suggest a geologically recent rupture. The second is the **Mangaone Anticline Fault**, which has been mapped from the western end of the Te Rimuomaru fault southwest to the edge of the LiDAR data. The fault is close to, but west of, the crest of the bedrock Mangaone Anticline (Mazengarb and Speden 2000). The total mapped length of the Mangaone Anticline Fault is ~7 km, but it could extend farther southwest into the Wairoa District. Many of these traces are very sharp (i.e. very distinct in the LiDAR data), which may also suggest a geologically recent rupture on this fault.

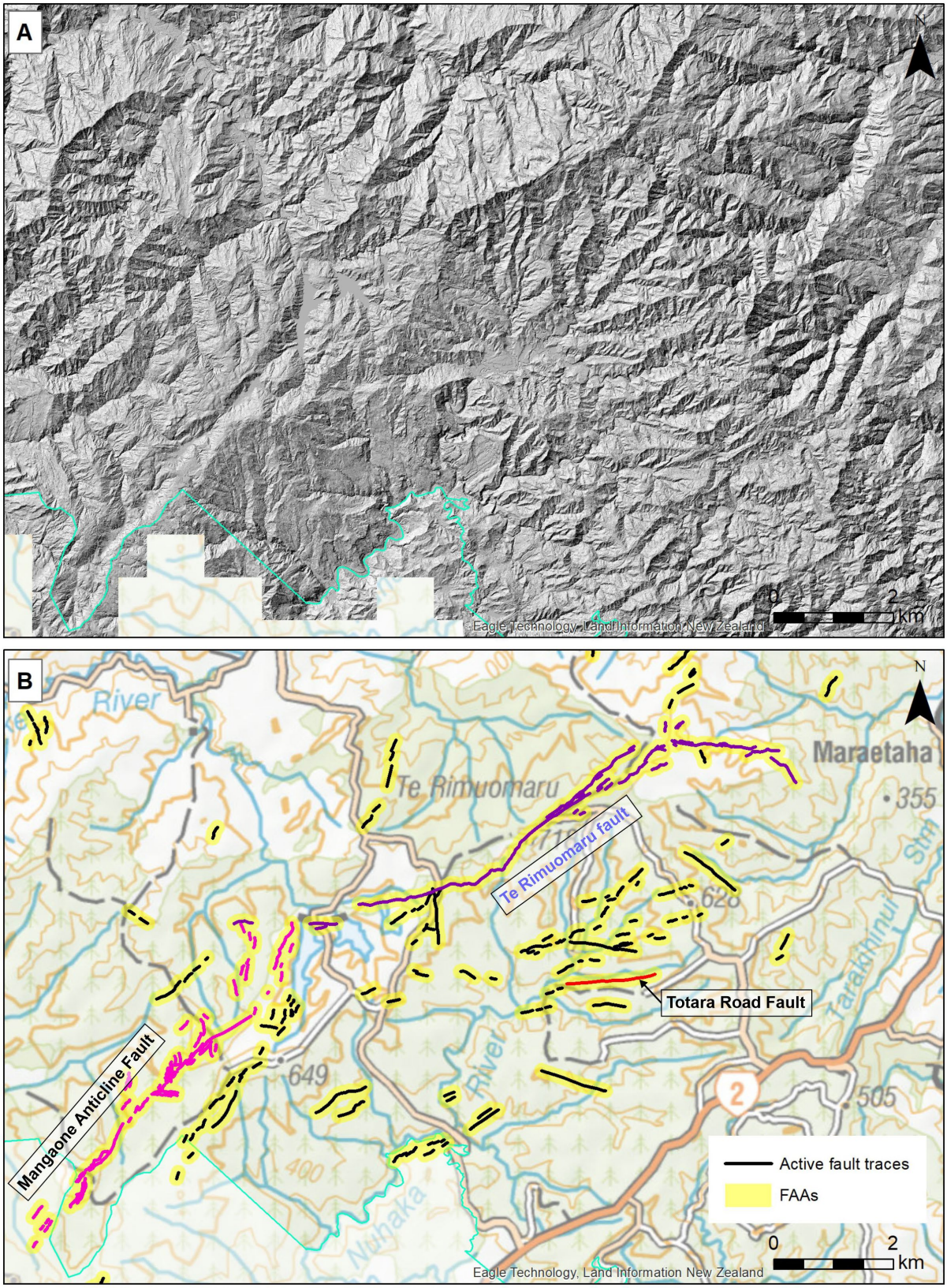

Figure 4.12 Faults southwest of Maraetaha. (a) LiDAR hillshade map (illuminated from the northwest). (b) Active fault traces and FAAs.

4.3.3 Previously Mapped Faults Now Not Regarded as Active

Two N–S-oriented active faults were previously mapped crossing the western edge of Tairāwhiti Gisborne District, the **Motu Fault** along the Motu River valley and the **Kotare Fault** ~16 km to the west of the Motu Fault (Figure 1.2). While these are clearly bedrock faults (Mazengarb and Speden 2000), it is not clear that active traces occur in Tairāwhiti Gisborne District. The southern end of the previously mapped active trace of the Motu Fault extended for ~8 km into the district, but, despite careful searching, we have found no clear traces on the hillsides or on the Motu River terraces on the LiDAR data. There are possible active fault traces of the Kotare Fault on the edge of the LiDAR data within the Ōpōtiki District, and another possible trace southeast of the previously-mapped Kotare Fault, but no traces across the river terraces in between. Because of this uncertainty, we do not assign these traces to the Kotare Fault. The absence of active fault traces on the Motu and Kotare faults in Tairāwhiti Gisborne District means that we do not include these in the active fault dataset but recommend that they are further examined when LiDAR data becomes available in the adjacent Ōpōtiki District.

The **Pangopango Fault** is a bedrock fault south of the Fernside Fault west of Anaura Bay (Figure 1.2) (Mazengarb and Speden 2000). Three short (≤240 m) traces have been mapped approximately along the previously mapped active fault (Figure 4.1). However, due to the short length and uncertainty in its tectonic origin, we consider that there is insufficient evidence to retain the Pangopango Fault as an active fault.

Active traces had previously been mapped along the eastern end of the bedrock **Arakihi Fault**, parallel to the Repongaere Fault, and the **Otoko-Totangi Fault**, which meets the eastern end of the Arakihi Fault (Figure 1.2) (Mazengarb and Speden 2000). There are no clear traces visible in the LiDAR data along the previously mapped traces of the Arakihi Fault, and only two short (≤130 m) possibly active fault traces have been mapped along the central Otoko-Totangi Fault (Figure 4.1). Some new traces have been mapped farther west, extending semi-continuously for ~7 km. However, these are not along the mapped Otoko-Totangi bedrock fault, therefore we leave them unnamed.

4.4 Newly Identified Faults (Priority 3)

Five sets of active fault traces are continuous enough to be considered newly identified active faults. One of these, the Te Rimuomaru fault, was described in Section 4.2 and the East Cape, Kahunui, Pukeopo and Smart Road faults are described from north to south below. These new faults are named with blue labels in Figure 4.1.

Possible active fault traces have been mapped along and west of the bedrock **East Cape Fault** (Figure 4.13). The westernmost traces are the clearest on the LiDAR data, and there do not appear to be any traces in the wide valleys of the Te Waiau or Te Parera streams. The southernmost trace is mapped along a step in the terrace on the north side of Waikākā Stream mouth, and it is possible that this is a river or marine terrace feature rather than a fault, so it is worthy of further investigation in order to verify, or not, its tectonic origin.

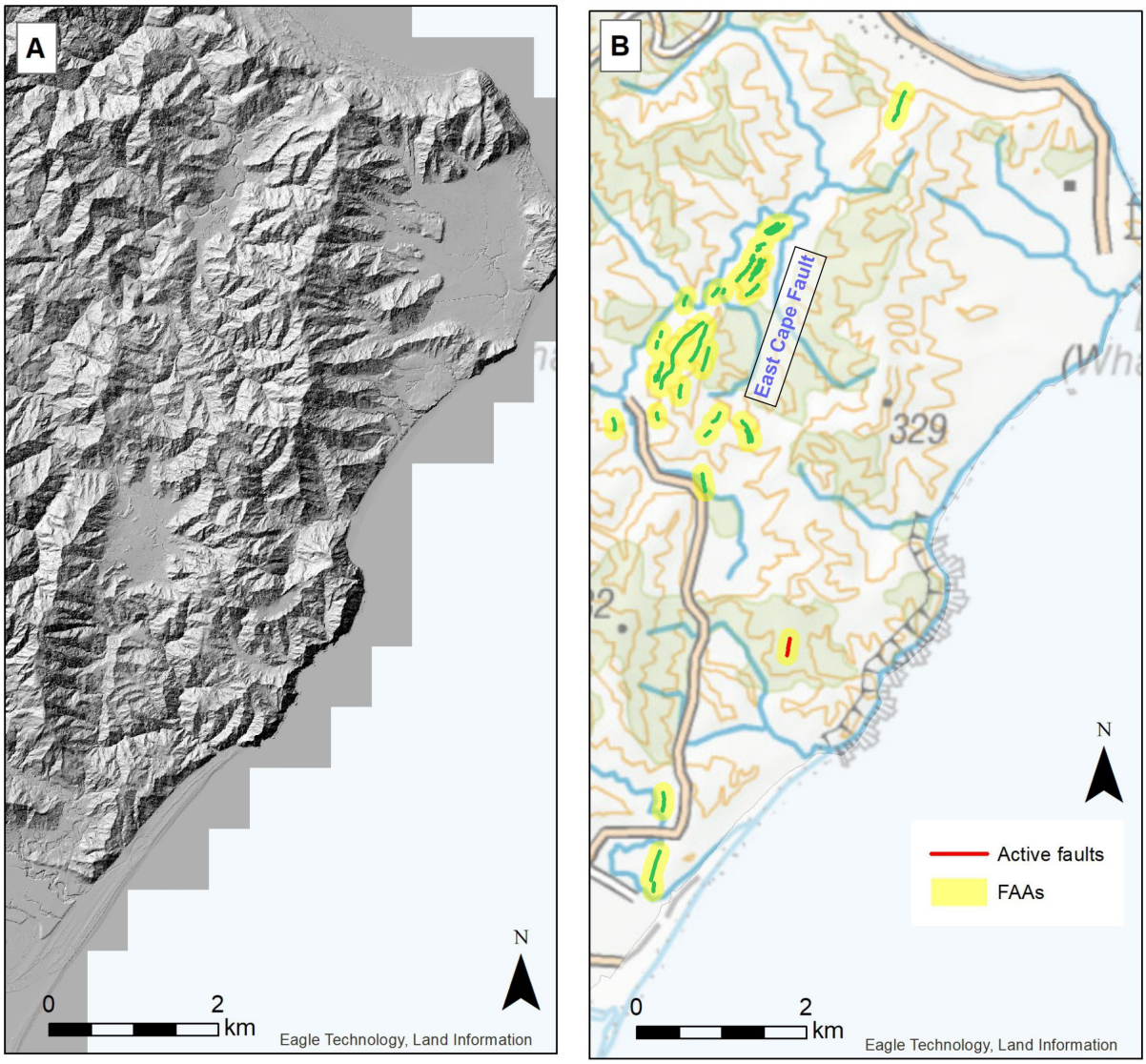

Figure 4.13 The East Cape Fault (green) and another possible active fault trace (red). (a) LiDAR hillshade map (illuminated from the northwest). (b) Active fault traces and FAAs.

The **Smart Road fault**, **Pukeopou fault** and **Kahunui fault** are in the west of Tairāwhiti Gisborne District, extending from near State Highway 2 in the north to the southern boundary of the district on Kahunui Ridge (Figure 4.14). Although there are gaps between each set of faults, each set is still relatively short (≤11 km), so it is possible that they are all the same fault and/or rupture together in the same earthquake. Large parts of each of these faults have very clear, sharp traces on the LiDAR data, which may suggest a geologically recent rupture. A short trace had previously been mapped along the Smart Road fault in the compilation of QMAP Raukumara, but the mapping in this study extends it to a total length of 11 km. The Pukeopou fault consists of continuous and clear 3-km-long set of traces on the northwest side of Pukeopou ridge. Another set of more distributed, less distinct, traces has been mapped to the northeast, which could potentially be a continuation of the Pukeopou fault, but, due to the differences in morphology, we leave these traces unnamed until further work is undertaken. The Kahunui fault is unusual in having a W–E orientation and also has very sharp traces along its entire mapped length (10 km). The Kahunui fault extends to the edge of the LiDAR data, so it likely extends beyond into the Wairoa District. However, there is no clear sign of it in Tairāwhiti Gisborne District west of the triangular gap, so, if it does continue for a significant distance, its orientation would likely swing to the south.

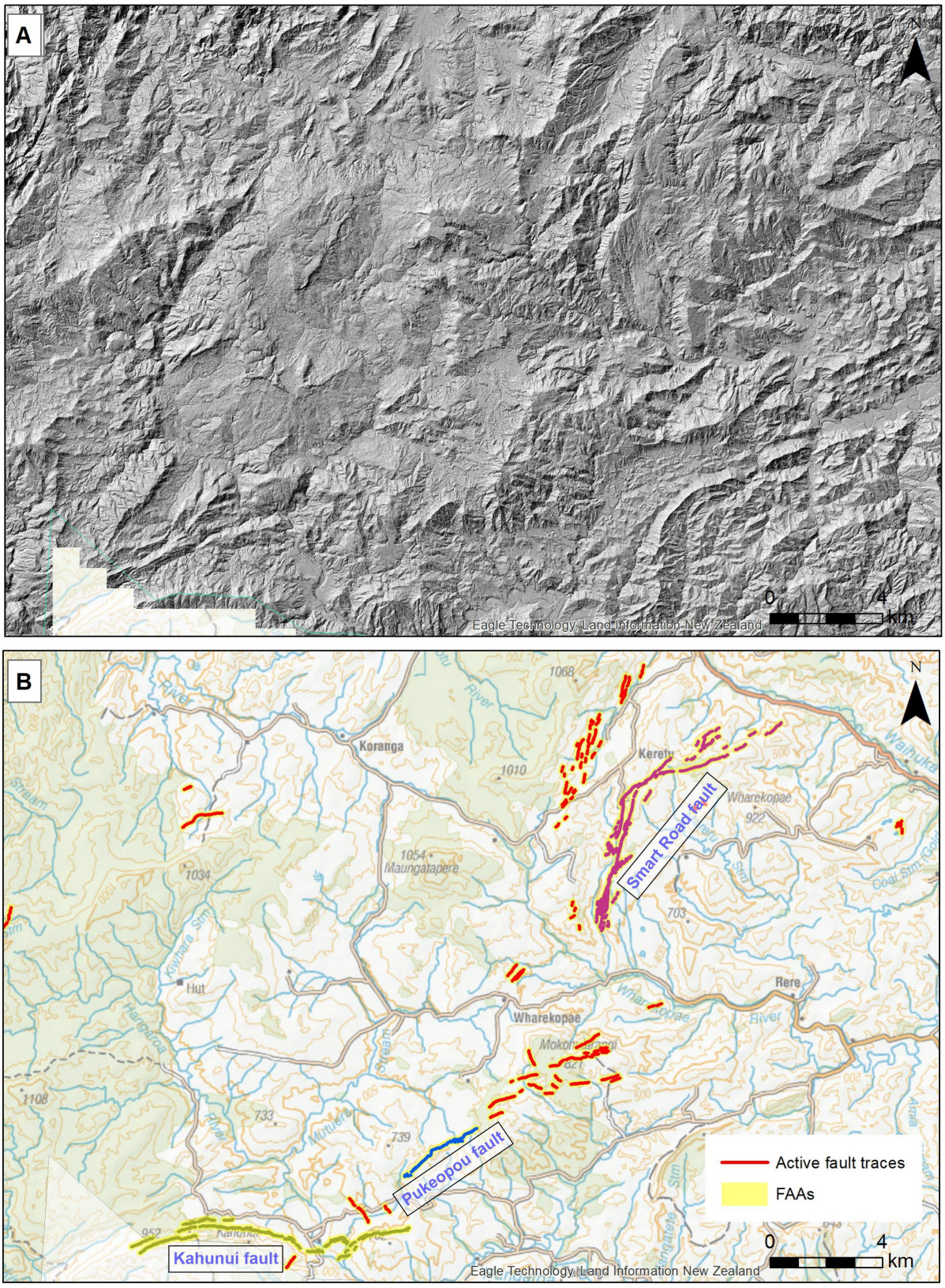

Figure 4.14 The Smart Road (purple), Pukeopou (blue) and Kahunui (yellow-green) faults. (a) LiDAR hillshade map (illuminated from the northwest). (b) Active fault traces and FAAs.

4.5 Critical Infrastructure (Priority 2) and Other Faults (Priority 3)

Of the named active faults in this study, only one fault, the Waihau Fault, crosses a state highway (Figure 4.11). Several short, possibly related, traces to the north also cross State Highway 2. As noted in Section 4.3.2, the short length and unusual distribution of the Waihau Fault and nearby traces means that their tectonic origin is ambiguous and some future investigations are therefore warranted. In addition to these named faults, the new possible, unnamed, fault in the Tolaga Bay priority area also crosses State Highway 35 in the town and was discussed in Section 4.2. Short, possible fault traces have been mapped close to or crossing State Highways 2 (near Rimu Hill) and 35 (north of Ruatoria; Figure 4.4).

No faults have been mapped crossing the water pipeline between Waterworks Bush and Gisborne City. However, as noted in Section 4.3.2, the western end of the Te Rimuomaru fault crosses the water supply reservoirs. Some further work, such as field mapping, could be undertaken to investigate their tectonic origin and to possibly determine timing of movement and recurrence interval, but geophysical (e.g. GPR) or paleoseismological (e.g. trenching) investigations would be challenging due to the bush cover and environmental considerations in the water-supply catchment.

Systematic mapping in the priority 3 areas identified a number of other, relatively short, traces that, in the main, have been assigned a Tectonic Origin of ‘possible’ (meaning that we suspect these traces could have their origin in fault movement, but there could be other explanations). The longest have been named and described in Sections 4.3.2 and 4.4. Of the rest, the clearest and most continuous are the W–N–W-oriented traces north of the Repongaere Fault and NW-oriented traces in the Parikanapa area ~30 km west of Gisborne (Figure 4.1).

Due to time constraints, no systematic mapping was undertaken outside the priority 3 areas. However, we think that it is unlikely that there are any major (>10-km-long) faults present in these areas.

5.0 SUMMARY AND RECOMMENDATIONS

5.1 Summary

Active faults have been mapped using LiDAR data in Tairāwhiti Gisborne District with particular focus on areas around towns, critical infrastructure and previously mapped faults. The mapping identified many short traces along many of the previously mapped faults and identified some previously unmapped faults/traces. All are short (≤11 km), which supports previous interpretations that they are likely secondary faults. Newly identified fault traces have been mapped crossing southern Tolaga Bay town, near Tokomaru Bay town, east of Ruatoria and crossing the water-supply reservoirs. Active traces were not mapped along five previously mapped faults, the Motu, Kotare, Pangopango, Arakihi and Otoko-Totangi faults, and these have been removed from the active fault dataset.

Recurrence interval information is only available for two faults, the Repongaere and Pakarae faults, which have been assigned to RI Classes III (>3500 to ≤5000 years) and II (>2000 to ≤3500 years), respectively, with medium confidence. FAZs have been developed for these two faults following the methodology detailed in the MfE Active Fault Guidelines. FAAs have been developed for the remaining faults by buffering the traces by 125 m either side of the mapped fault (total width 250 m).

A trial was undertaken of a semi-automated fault-mapping tool (edge detection) on selected areas in Tairāwhiti Gisborne District. In general, the results did not successfully reproduce the accuracy or level of detail required for active fault mapping that can be obtained using manual mapping, due to the steep topography and relatively subtle topographic expressions of many of the faults. Some success was gained by altering parameters for specific site locations, but the extra supervision currently required means that it is not efficient enough to scale up to use this tool across the entire district.

5.2 Recommendations

Based on the findings of the trial of the semi-automated edge-detection mapping tool in Tairāwhiti Gisborne District, we suggest a number of possible improvements or alternatives to aid in the development of such tools:

- Mask ridgelines, deeply incised river valleys and known landslides from the LiDAR dataset so that they do not influence edge-detection results.
- Develop ways to automatically adjust the threshold value used by the Canny Edge Detection algorithm.
- Investigate the use of scale-dependence.
- Investigate other tools, such as those that use deep-learning-based methodologies.

Based on the findings of the manual mapping in this report, GNS Science recommends that Te Kaunihera o Te Tairāwhiti Gisborne District Council:

- Replace any Tairāwhiti Gisborne District active fault datasets with those from this study.
- Develop planning provisions using the information provided in this report, including guiding principles and the risk-based decision-making tools in the MfE Active Fault Guidelines and ECan FAA Guidelines.
- Include the FAZs and FAAs in the Gisborne District Plan.

- Investigate the tectonic origin of, and RI Class information for, faults mapped in the vicinity of Tolaga Bay, Tokomaru Bay, Ruatoria and the water-supply reservoirs. This could be achieved through a combination of field mapping, geophysical surveys (e.g. GPR) and paleoseismic trenching studies.
- Socialise (e.g. communicate with stakeholders) the information in this report.

6.0 ACKNOWLEDGEMENTS

We would like to thank Chris Massey for preliminary discussions on distinguishing faults and landslides and Genevieve Coffey and Russ Van Dissen for their reviews of this report.

7.0 REFERENCES

Alloway BV, Lowe DJ, Barrell DJA, Newnham RM, Almond PC, Augustinus PC, Bertler NAN, Carter L, Litchfield NJ, McGlone MS, et al. 2007. Towards a climate event stratigraphy for New Zealand over the past 30,000 years (NZ-INTIMATE project). *Journal of Quaternary Science*. 22(1):9–35. doi:10.1002/jqs.1079.

[ANR] Agence Nationale de la Recherche. 2018. Hope Fault, NZ 2010. Paris (FR): ANR; [accessed 2022 Oct 30]. https://doi.org/10.5069/G93J3B2J

Barnes PM. 1994. Continental extension of the Pacific Plate at the southern termination of the Hikurangi subduction zone: the North Mernoo Fault Zone, offshore New Zealand. *Tectonics*. 13(4):735–754. doi:10.1029/94TC00798.

Barnes PM, Audru JC. 1999. Quaternary faulting in the offshore Flaxbourne and Wairarapa Basins, southern Cook Strait, New Zealand. *New Zealand Journal of Geology and Geophysics*. 42(3):349–367. doi:10.1080/00288306.1999.9514851.

Barnes PM, Lamarche G, Bialas J, Henrys S, Pecher I, Netzeband G, Greinert J, Mountjoy J, Pedley K, Crutchley G. 2010. Tectonic and geological framework for gas hydrates and cold seeps on the Hikurangi Subduction Margin, New Zealand. *Marine Geology*. 272(1–4):26–48. doi:10.1016/j.margeo.2009.03.012.

Barnes PM, Nicol A, Harrison T. 2002. Late Cenozoic evolution and earthquake potential of an active listric thrust complex above the Hikurangi subduction zone, New Zealand. *Geological Society of America Bulletin*. 114(11):1379–1405. doi:10.1130/0016-7606(2002)114<1379:Lceaep>2.0.Co;2.

Barrell DJA. 2013. General distribution and characteristics of active faults and folds in the Selwyn District, North Canterbury. Dunedin (NZ): GNS Science. 53 p. Consultancy Report 2012/325. Prepared for Environment Canterbury.

Barrell DJA. 2019. General distribution and characteristics of active faults and folds in the Queenstown Lakes and Central Otago districts, Otago. Dunedin (NZ): GNS Science. 99 p. Consultancy Report 2018/207. Prepared for Otago Regional Council.

Barrell DJA, Jack H, Gadsby M. 2015. Guidelines for using regional-scale earthquake fault information in Canterbury. Dunedin (NZ): GNS Science. 30 p. Consultancy Report 2014/211. Prepared for Canterbury Regional Council (Environment Canterbury).

Barrell DJA, Townsend DB. 2012. General distribution and characteristics of active faults and folds in the Hurunui District, North Canterbury. Dunedin (NZ): GNS Science. 30 p. + 1 CD. Consultancy Report 2012/113. Prepared for Environment Canterbury.

Beauprêtre S, Garambois S, Manighetti I, Malavieille J, Sénéchal G, Chatton M, Davies T, Larroque C, Rousset D, Cotte N, et al. 2012. Finding the buried record of past earthquakes with GPR-based palaeoseismology: a case study on the Hope fault, New Zealand. *Geophysical Journal International*. 189(1):73–100. doi:10.1111/j.1365-246X.2012.05366.x.

Berryman KR, Marden M, Palmer A, Litchfield NJ. 2009. Holocene rupture of the Repongaere Fault, Gisborne: implications for Raukumara Peninsula deformation and impact on the Waipaoa Sedimentary System. *New Zealand Journal of Geology and Geophysics*. 52(4):335–347. doi:10.1080/00288306.2009.9518462.

Bradski GR, Kaehler A. 2008. Learning OpenCV: computer vision with the OpenCV library. Sebastopol (CA): O'Reilly Media, Inc. 555 p.

Canny J. 1986. A computational approach to edge detection. *IEEE Transactions on Pattern Analysis and Machine Intelligence.* PAMI-8(6):679–698. doi:10.1109/TPAMI.1986.4767851.

Clark KJ, Ries WF. 2016. Mapping of active faults and fault avoidance zones for Wairoa District: 2016 update. Lower Hutt (NZ): GNS Science. 35 p. + 1 DVD. Consultancy Report 2016/133. Prepared for Hawke's Bay Regional Council.

Clement AJH, Whitehouse PL, Sloss CR. 2016. An examination of spatial variability in the timing and magnitude of Holocene relative sea-level changes in the New Zealand archipelago. *Quaternary Science Reviews*. 131:73–101. doi:10.1016/j.quascirev.2015.09.025.

Duda RO, Hart PE. 1972. Use of the Hough transformation to detect lines and curves in pictures. *Communications of the ACM.* 15(1):11–15. doi:10.1145/361237.361242.

Francis DA. 1983. The Marau Beach Fault: an active fault in Z16 [map]. 7 p. Located at GNS Science, Lower Hutt, NZ; Z16/71

Francis DA. 1984. A zone of active faults in the Maraetaha-Mangaone area south-west of Gisborne. 8 p. + 2 figs. Located at GNS Science, Lower Hutt, NZ; 831/4.

Gage M, Black RD. 1979. Slope-stability and geological investigations at Mangatu State Forest. Wellington (NZ): New Zealand Forest Service, Forest Research Institute. 37 p. (Technical Paper; 66).

Grant Ludwig L, Akciz SO, Arrowsmith JR, Salisbury JB. 2019. Reproducibility of San Andreas Fault slip rate measurements at Wallace Creek in the Carrizo Plain, CA. *Earth and Space Science*. 6(1):156–165. doi:10.1029/2017EA000360.

Hicks DM, Hill J, Shankar U. 1996. Variation of suspended sediment yields around New Zealand: the relative importance of rainfall and geology. In: Walling DE, Webb BE, editors. *Erosion and sediment yield – global and regional perspectives: proceedings of an international symposium*; 1996 July 15–19; Exeter, United Kingdom. Wallingford (GB): International Association of Hydrological Sciences. p. 149–156. (IAHS publication; 236).

Hough PVC. 1959. Machine analysis of bubble chamber pictures. In: *Proceedings: 2nd International Conference on High-Energy Accelerators and Instrumentation*; 1959 Sep 14–19; Geneva, Switzerland. Geneva (CH): CERN. p. 554–558.

Jongens R, Dellow GD. 2003. The active faults database of NZ: data dictionary. Lower Hutt (NZ): Institute of Geological & Nuclear Sciences. 27 p. (Institute of Geological & Nuclear Sciences science report; 2003/17).

Kerr J, Nathan S, Van Dissen RJ, Webb P, Brunsdon D, King AB. 2003. Planning for development of land on or close to active faults: a guideline to assist resource management planners in New Zealand. Lower Hutt (NZ): Institute of Geological & Nuclear Sciences. 71 p. Client Report 2002/124. Prepared for the Ministry for the Environment.

King AB, Brunsdon DR, Shephard RB, Kerr JE, Van Dissen RJ. 2003. Building adjacent to active faults: a risk-based approach. In: *Proceedings of the 2003 Pacific Conference on Earthquake Engineering*; 2003 Feb 13–15; Christchurch, New Zealand. Wellington (NZ): New Zealand Society for Earthquake Engineering. Paper 158.

Langridge RM, Morgenstern R. 2019. Active fault mapping and fault avoidance zones for Horowhenua District and Palmerston North City. Lower Hutt (NZ): GNS Science. 72 p. Consultancy Report 2018/75. Prepared for Horizons Regional Council.

Langridge RM, Morgenstern R. 2020a. Active fault mapping and fault avoidance zones for the Manawatū District. Lower Hutt (NZ): GNS Science. 69 p. Consultancy Report 2019/123. Prepared for Horizons Regional Council.

Langridge RM, Morgenstern R. 2020b. Active fault mapping and fault avoidance zones for the Rangitikei District. Lower Hutt (NZ): GNS Science. 66 p. Consultancy Report 2019/168. Prepared for Horizons Regional Council.

Langridge RM, Morgenstern R, Coffey GL. 2021. Active fault mapping for planning purposes across the western part of the Tararua District. Lower Hutt (NZ): GNS Science. 85 p. Consultancy Report 2021/03. Prepared for Horizons Regional Council.

Langridge RM, Ries WF. 2014. Active fault mapping and fault avoidance zones for Central Hawke's Bay District: 2013 update. Lower Hutt (NZ): GNS Science. 50 p. + 1 CD. Consultancy Report 2013/151. Prepared for Hawke's Bay Regional Council.

Langridge RM, Ries WF. 2016. Active fault mapping and fault avoidance zone for the Wairau Fault, Marlborough District. Lower Hutt (NZ): GNS Science 49 p. + 1 DVD. Consultancy Report 2016/25. Prepared for Marlborough District Council.

Langridge RM, Ries WF, Litchfield NJ, Villamor P, Van Dissen RJ, Barrell DJA, Rattenbury MS, Heron DW, Haubrock S, Townsend DB, et al. 2016. The New Zealand Active Faults Database. *New Zealand Journal of Geology and Geophysics*. 59(1):86–96. doi:10.1080/00288306.2015.1112818.

Leonard GS, Begg JG, Wilson CJN, compilers. 2010. Geology of the Rotorua area [map]. Lower Hutt (NZ): GNS Science. 1 folded map + 102 p., scale 1:250,000. (Institute of Geological & Nuclear Sciences 1:250,000 geological map; 5).

Litchfield NJ, Clark KJ, Cochran UA, Palmer AS, Mountjoy J, Mueller C, Morgenstern R, Berryman KR, McFadden BG, Steele R, et al. 2020a. Marine terraces reveal complex near-shore upper-plate faulting in the northern Hikurangi Margin, New Zealand. *Bulletin of the Seismological Society of America*. 110(2):825–849. doi:10.1785/0120190208.

Litchfield NJ, Coffey GL, Morgenstern R. 2022. Active fault mapping for the South Wairarapa, Carterton and Masterton districts. Lower Hutt (NZ): GNS Science. 59 p. Consultancy Report 2021/117. Prepared for Greater Wellington Regional Council.

Litchfield N, Ellis S, Berryman K, Nicol A. 2007. Insights into subduction-related uplift along the Hikurangi Margin, New Zealand, using numerical modeling. *Journal of Geophysical Research: Earth Surface*. 112(F2). doi:10.1029/2006jf000535.

Litchfield NJ, Morgenstern R, Van Dissen RJ, Langridge RM, Pettinga JR, Jack H, Barrell DJA, Villamor P. 2019. Updated assessment of active faults in the Kaikōura District. Lower Hutt (NZ): GNS Science. 71 p. Consultancy Report 2018/141. Prepared for Canterbury Regional Council (Environment Canterbury).

Litchfield NJ, Morgenstern R, Villamor P, Van Dissen RJ, Townsend DB, Kelly SD. 2020b. Active fault hazards in the Taupō District. Lower Hutt (NZ): GNS Science. 114 p. Consultancy Report 2020/31. Prepared for Taupō District Council.

Litchfield NJ, Van Dissen RJ. 2014. Porirua District fault trace study. Lower Hutt (NZ): GNS Science. 53 p. Consultancy Report 2014/213. Prepared for Greater Wellington Regional Council; Porirua Council.

Marden M, Fuller IC, Herzig A, Betts HD. 2018. Badass gullies: fluvio-mass-movement gully complexes in New Zealand's East Coast region, and potential for remediation. *Geomorphology*. 307:12–23. doi:10.1016/j.geomorph.2017.11.012.

Marden M, Mazengarb C, Palmer A, Berryman K, Rowan D. 2008. Last glacial aggradation and postglacial sediment production from the non-glacial Waipaoa and Waimata catchments, Hikurangi Margin, North Island, New Zealand. *Geomorphology*. 99(1–4):404–419. doi:10.1016/j.geomorph.2007.12.003.

Mattéo L, Manighetti I, Tarabalka Y, Gaucel J-M, van den Ende M, Mercier A, Tasar O, Girard N, Leclerc F, Giampetro T, et al. 2021. Automatic fault mapping in remote optical images and topographic data with deep learning. *Journal of Geophysical Research: Solid Earth*. 126(4):e2020JB021269. doi:10.1029/2020JB021269.

Mazengarb C. 1984. The Fernside Fault: an active normal fault, Raukumara Peninsula, New Zealand. In: Gilchrist C, editor. *Research notes 1984*. Lower Hutt (NZ): New Zealand Geological Survey. p. 98–103. (New Zealand Geological Survey record; 3).

Mazengarb C, Francis DA, Moore PR. 1991. Tauwhareparae [map]. Lower Hutt (NZ): New Zealand Geological Survey. 1 fold. map + 1 booklet, scale 1:50,000. (Geological map of New Zealand 1:50,000; sheet Y16).

Mazengarb C, Speden IG. 2000, compilers. Geology of the Raukumara area [map]. Lower Hutt (NZ): Institute of Geological & Nuclear Sciences Limited. 1 map + 60 p., scale 1:250,000. (Institute of Geological & Nuclear Sciences 1:250,000 geological map; 6).

Mountjoy JJ, Barnes PM. 2011. Active upper plate thrust faulting in regions of low plate interface coupling, repeated slow slip events, and coastal uplift: example from the Hikurangi Margin, New Zealand. *Geochemistry, Geophysics, Geosystems*. 12(1):Q01005. doi:10.1029/2010gc003326.

Mountjoy JJ, Barnes PM, Pettinga JR. 2009. Morphostructure and evolution of submarine canyons across an active margin: Cook Strait sector of the Hikurangi Margin, New Zealand. *Marine Geology*. 260(1–4):45–68. doi:10.1016/j.margeo.2009.01.006.

[NCALM] National Center for Airborne Laser Mapping. 2006. B4 Project: Southern San Andreas and San Jacinto Faults. Houston (TX): NCALM; [accessed 2022 Oct 26]. https://doi.org/10.5069/G97P8W9T

Nodder S, Lamarche G, Proust J-N, Stirling M. 2007. Characterizing earthquake recurrence parameters for offshore faults in the low-strain, compressional Kapiti-Manawatu Fault System, New Zealand. *Journal of Geophysical Research: Solid Earth*. 112:B12102. doi:10.1029/2007JB005019.

Ota Y, Hull AG, Berryman KR. 1991. Coseismic uplift of Holocene marine terraces in the Pakarae River area, Eastern North Island, New Zealand. *Quaternary Research*. 35(3):331–346. doi:10.1016/0033-5894(91)90049-b.

Pondard N, Barnes PM. 2010. Structure and paleoearthquake records of active submarine faults, Cook Strait, New Zealand: implications for fault interactions, stress loading, and seismic hazard. *Journal of Geophysical Research: Solid Earth*. 115(B12):B12320. doi:10.1029/2010jb007781.

Sare R, Hilley GE. 2018. Scarplet: a Python package for topographic template matching and diffusion dating. *Journal of Open Source Software*. 3(31):1066. doi:10.21105/joss.01066.

Scott CP, Giampietro T, Brigham C, Leclerc F, Manighetti I, Arrowsmith JR, Laó-Dávila DA, Mattéo L. 2022. Semiautomatic algorithm to map tectonic faults and measure scarp height from topography applied to the Volcanic Tablelands and the Hurricane Fault, Western US. *Lithosphere*. 2021(Special 2):9031662. doi:10.2113/2021/9031662.

Seebeck H, Van Dissen RJ, Litchfield NJ, Barnes PM, Nicol A, Langridge RM, Barrell DJA, Villamor P, Ellis SM, Rattenbury MS, et al. 2022. New Zealand Community Fault Model – version 1.0. Lower Hutt (NZ): GNS Science. 97 p. (GNS Science report; 2021/57). doi:10.21420/GA7S-BS61.

Stirling M, McVerry G, Gerstenberger M, Litchfield N, Van Dissen RJ, Berryman K, Barnes P, Wallace L, Villamor P, Langridge R, et al. 2012. National Seismic Hazard Model for New Zealand: 2010 update. *Bulletin of the Seismological Society of America*. 102(4):1514–1542. doi:10.1785/0120110170.

Thornley S. 1996. Neogene tectonics of Raukumara Peninsula, northern Hikurangi margin, New Zealand [PhD thesis]. Wellington (NZ): Victoria University of Wellington. 291 p.

Van Dissen RJ, Heron DW. 2003. Earthquake fault trace survey, Kapiti Coast District. Lower Hutt (NZ): Institute of Geological & Nuclear Sciences. 45 p. Client Report 2003/77. Prepared for Kāpiti Coast District Council.

Van Dissen RJ, Litchfield NJ, Begg JG. 2005. Upper Hutt City fault trace project. Lower Hutt (NZ): Institute of Geological & Nuclear Sciences. 28 p. Client Report 2005/151. Prepared for Greater Wellington Regional Council, Upper Hutt City Council.

Villamor P, Berryman KR. 2001. A Late Quaternary extension rate in the Taupo Volcanic Zone, New Zealand, derived from fault slip data. *New Zealand Journal of Geology and Geophysics*. 44(2):243–269. doi:10.1080/00288306.2001.9514937.

Wallace LM, Barnes P, Beavan J, Van Dissen R, Litchfield N, Mountjoy J, Langridge R, Lamarche G, Pondard N. 2012. The kinematics of a transition from subduction to strike-slip: an example from the central New Zealand plate boundary. *Journal of Geophysical Research: Solid Earth*. 117:B02405. doi:10.1029/2011jb008640.

Wilson KJ, Berryman KR, Litchfield NJ, Little T. 2006. A revision of mid-late Holocene marine terrace distribution and chronology at the Pakarae River mouth, North Island, New Zealand. *New Zealand Journal of Geology and Geophysics*. 49(4):477–489. doi:10.1080/00288306.2006.9515182.

APPENDICES

This page left intentionally blank.

APPENDIX 1 ACTIVE FAULT DEFINITIONS

A1.1 What is an Active Fault?

Active faults are those faults considered capable of generating strong earthquake shaking and ground-surface fault rupture, causing significant damage.[4] Ground-surface-rupturing earthquakes are typically of magnitude M_W >6.5.[5]

An active fault in Aotearoa New Zealand is generally defined as one that has deformed the ground surface within the past 125,000 years (Langridge et al. 2016). This is defined in part, for practical reasons, as those faults that deform marine terraces and alluvial surfaces that formed during the 'Peak Last Interglacial period' or Marine Isotope Stage (MIS) 5e or younger (MIS 1–4; e.g. Alloway et al. 2007). The exception to this definition is the Taupō Rift, which is considered to be evolving so quickly that an active fault is defined as one that has deformed the ground surface within the past 25,000 years (Villamor and Berryman 2001; Langridge et al. 2016).

The purpose of this appendix is to introduce how active faults express themselves, i.e. their behaviour, styles of deformation, activity and geomorphic expression. Active faults are typically expressed in the landscape as linear traces displacing surficial geologic features, which may include hillslopes, alluvial terraces and fans. The age of these displaced features can be used to define how active a fault is.

Active faults are often defined by a fault scarp or trace. A fault scarp is formed when a fault displaces or deforms the land surface or seafloor and produces an abrupt linear step, which smooths out with time to form a scarp (Figure A1.1). In some cases, where a fault moves horizontally, only a linear trace or furrow may be observed.

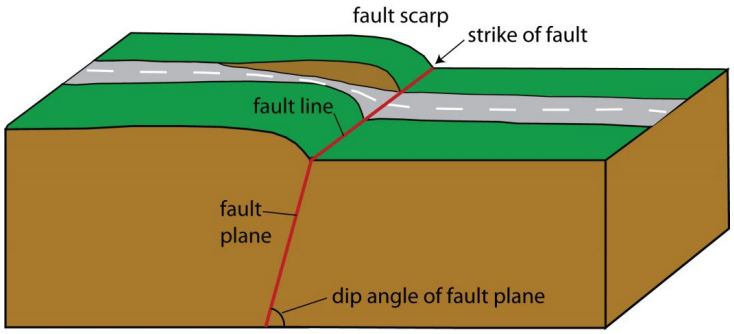

Figure A1.1 Block model of a generic active fault. Fault displacement produces a scarp along the projection of the fault plane at the Earth's surface (fault line or trace).

A1.2 Sense of Fault Movement

Faults can be categorised as dip-slip faults, where the dominant sense of motion is vertical (defined by movement in the dip, or inclination, direction of the fault), and strike-slip faults, where the dominant sense of movement is horizontal (movement in the strike direction of the fault).

4 A fault is a plane that separates two bodies of rock, whereby one side moves relative to the other side. A fault differs from a fracture, which has no movement across it. Faults can extend metres to kilometres into the Earth.

5 Surface rupture can also occur during smaller earthquakes when the earthquake epicentre is relatively close to the Earth's surface or, locally, from triggered slip from another nearby surface fault-rupture earthquake.

Dip-slip faults can be divided into normal faults, formed under extension (where the hanging-wall block of the fault drops down; Figure A1.3), and reverse faults, formed mainly under contraction (where the hanging-wall block of the fault is pushed up; Figure A1.4). Thrust faults are a subset of shallow-dipping (inclined) reverse faults. The majority of faults in Tairāwhiti Gisborne District are considered to be normal faults, but a few possible reverse faults have also been identified. Active faults offshore to the east of the Tairāwhiti coast are mostly thrust faults.

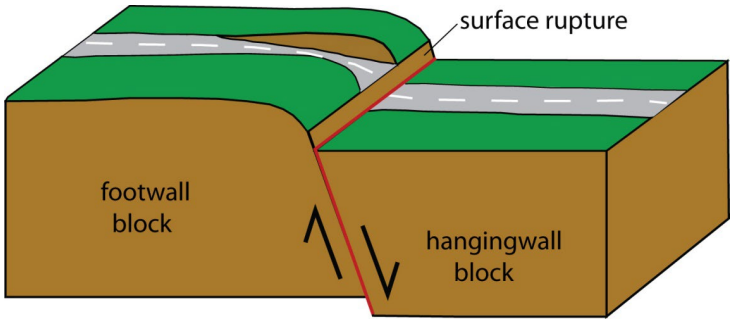

Figure A1.2 Block model of a normal dip-slip fault. The relative movement of the blocks is vertical and in the dip direction of the fault plane. The hanging-wall block has dropped down, enhancing the height of the fault scarp.

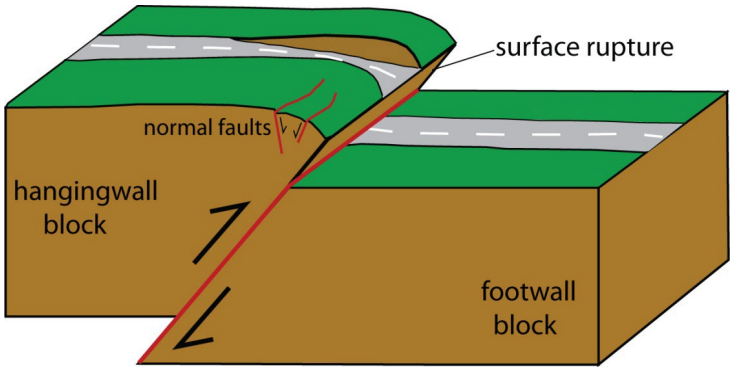

Figure A1.3 Block model of a reverse dip-slip fault that has recently ruptured. Movement of the blocks is vertical and in the dip direction of the fault plane. In this case, the hanging-wall block has been pushed up over the footwall block. Folding and normal faulting are common features of deformation in the hanging-wall block of reverse faults.

Strike-slip faults are defined as either right-lateral (dextral), where the motion on the opposite side of the fault is to the right (Figure A1.2), or left-lateral (sinistral), where the opposite side of the fault moves to the left. There are some possible strike-slip faults in the Tairāwhiti Gisborne District, but they are more common west of Tairāwhiti Gisborne District, in the North Island Dextral Fault Belt or North Island Fault System, which extends from Wellington to the Bay of Plenty (Figure A1.1).

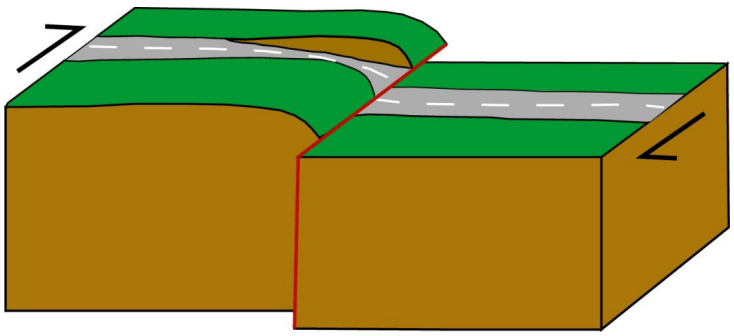

Figure A1.4 Block model of a strike-slip fault (red line). The fault is a right-lateral (dextral) fault, as shown by the black arrows and the sense of movement across the two blocks and a right separation across the road.

APPENDIX 2 FAULT AVOIDANCE ZONE BUILDING IMPORTANCE CATEGORY AND RECURRENCE INTERVAL CLASS

A2.1 Building Importance Category

In the event of fault rupture, buildings constructed across the fault will experience significant stress and can suffer extensive damage. Buildings adjacent to the fault and within the Fault Avoidance Zone (FAZ) may also be damaged. The MfE Active Fault Guidelines define five Building Importance Categories (Table A2.1) based on accepted risk levels for building collapse considering building type, use and occupancy. This categorisation is weighted toward life safety, but also allows for the importance of critical structures and the need to locate these wisely.

Table A2.1 Building Importance Categories from the MfE Active Fault Guidelines (Kerr et al. 2003).

Building Importance Category	Description	Examples
1	**Temporary structures** with low hazard to life and other property	• Structures with a floor area of <30 m^2 • Farm buildings, fences • Towers in rural situations
2a	**Timber-framed** residential construction	• Timber-framed single-storey dwellings
2b	**Normal structures** and structures not in other categories	• Timber-framed houses with area >300 m^2 • Houses outside the scope of NZS 3604 'Timber-Framed Buildings' • Multi-occupancy residential, commercial and industrial buildings accommodating <5000 people and <10,000 m^2 • Public assembly buildings, theatres and cinemas <1000 m^2 • Car parking buildings
3	**Important structures** that may contain people in crowds or contents of high value to the community or pose risks to people in crowds	• Emergency medical and other emergency facilities not designated as critical post-disaster facilities • Airport terminals, principal railway stations, schools • Structures accommodating >5000 people • Public assembly buildings >1000 m^2 • Covered malls >10,000 m^2 • Museums and art galleries >1000 m^2 • Municipal buildings • Grandstands >10,000 people • Service stations • Chemical storage facilities >500 m^2
4	**Critical structures** with special post-disaster functions	• Major infrastructure facilities • Air traffic control installations • Designated civilian emergency centres, medical emergency facilities, emergency vehicle garages, fire and police stations

A2.2 Relationship between RI Class and Building Importance Category

The MfE Active Fault Guidelines advocate a risk-based approach to dealing with development of land on, or close to, active faults. The risk is a function not only of the location and activity of a fault but also of the type of structure/building that may be impacted by rupture of the fault. For a site on or immediately adjacent to an active fault, risk increases both as fault activity increases (i.e. fault recurrence interval and Recurrence Interval Class decrease) and Building Importance Category increases. In order to maintain a relatively constant/consistent level of risk throughout the district, it appears reasonable to impose more restrictions on the development of sites located on or immediately adjacent to highly active faults, compared to sites located on or immediately adjacent to low-activity faults. This hierarchical relationship between fault activity (Recurrence Interval Class) and building type (Building Importance Category) is presented in Table A2.2.

The MfE Active Fault Guidelines also make a pragmatic distinction between previously subdivided and/or developed sites and undeveloped 'greenfield' sites and allows for different conditions to apply to these two types of sites of differing development status (see Table A2.2). The rationale for this is that, in the subdivision/development of a greenfield area, a change of land usage is usually being sought, and it is much easier, for example, to require a building setback distance from an active fault or to plan subdivision of land around the location of an active fault. However, in built-up areas, buildings may have been established without knowledge of the existence or location of an active fault, and the community may have an expectation to continue to live there, despite the potential danger. Also, existing use rights under the Resource Management Act mean that, where an existing building over a fault is damaged, it can be rebuilt, even after the hazard/risk has been identified.

Table A2.2 Relationships between Recurrence Interval Class, average recurrence interval of surface rupture, and Building Importance Category for previously subdivided and greenfield sites. For more details, see Kerr et al. (2003) and King et al. (2003).

<table>
<tr><th rowspan="2">Recurrence Interval Class</th><th rowspan="2">Average Recurrence Interval of Surface Rupture</th><th colspan="2">Building Importance (BI) Category Limitations (Allowable Buildings)</th></tr>
<tr><th>Previously Subdivided or Developed Sites</th><th>‘Greenfield’ Sites</th></tr>
<tr><td>I</td><td>≤2000 years</td><td>BI Category 1
Temporary buildings only</td><td rowspan="2">BI Category 1
Temporary buildings only</td></tr>
<tr><td>II</td><td>>2000 years to ≤3500 years</td><td>BI Category 1 and 2a
Temporary and residential timber-framed buildings only</td></tr>
<tr><td>III</td><td>>3500 years to ≤5000 years</td><td>BI Category 1, 2a and 2b
Temporary, residential timber-framed and normal structures</td><td>BI Category 1 and 2a
Temporary and residential timber-framed buildings only</td></tr>
<tr><td>IV</td><td>>5000 years to ≤10,000 years</td><td rowspan="2">BI Category 1, 2a, 2b and 3
Temporary, residential timber-framed, normal and important structures (but not critical post-disaster facilities)</td><td>BI Category 1, 2a and 2b
Temporary, residential timber-framed and normal structures</td></tr>
<tr><td>V</td><td>>10,000 years to ≤20,000 years</td><td>BI Category 1, 2a, 2b and 3
Temporary, residential timber-framed, normal and important structures (but not critical post-disaster facilities)</td></tr>
<tr><td>VI</td><td>>20,000 years to ≤125,000 years</td><td colspan="2">BI Category 1, 2a, 2b, 3 and 4
Critical post-disaster facilities cannot be built across an active fault with a recurrence interval of ≤20,000 years</td></tr>
</table>

Note: Faults with average recurrence intervals >125,000 years are not considered active.

APPENDIX 3 EXAMPLES OF RESOURCE CONSENT CATEGORY TABLES

Tables A3.1 and A3.2 present examples of relationships between Resource Consent Category, Building Importance Category, fault Recurrence Interval Class and Fault Complexity for both previously developed and greenfield sites along faults with FAZs in Tairāwhiti Gisborne District. These examples are modified from the MfE Active Fault Guidelines based on recommendations made for a similar fault mapping study for the Kāpiti Coast District Council (Van Dissen and Heron 2003). Table A3.3 shows recommended actions for activities within the Fault Awareness Areas.

Table A3.1 Example of relationships between Resource Consent Category, Building Importance Category, fault Recurrence Interval Class and Fault Complexity for developed and/or already subdivided sites, based on the MfE Active Fault Guidelines (Kerr et al. 2003).

Developed and/or Already Subdivided Sites					
PAKARAE FAULT (based on fault Recurrence Interval Class II, >2000 years to ≤3500 years)					
Building Importance Category	**1**	**2a**	**2b**	**3**	**4**
Fault Complexity	**Resource Consent Category**				
Well defined and well-defined extended	Permitted	Permitted*	*Non-Complying*	*Non-Complying*	Prohibited
Distributed and uncertain constrained	Permitted	Permitted	*Discretionary*	*Non-Complying*	Non-Complying
Uncertain poorly constrained	Permitted	Permitted	*Discretionary*	*Non-Complying*	Non-Complying
REPONGAERE FAULT (based on fault Recurrence Interval Class III, >3500 years to ≤5000 years)					
Building Importance Category	**1**	**2a**	**2b**	**3**	**4**
Fault Complexity	**Resource Consent Category**				
Well defined and well-defined extended	Permitted	Permitted*	Permitted*	*Non-Complying*	Non-Complying
Distributed and uncertain constrained	Permitted	Permitted	Permitted	*Discretionary*	Non-Complying
Uncertain poorly constrained	Permitted	Permitted	Permitted	*Discretionary*	Non-Complying

Notes:

* Indicates that the Resource Consent Category is permitted but could be controlled or discretionary, given that the fault location is well defined.

Italics: The use of italics indicates that the Resource Consent Category of these categories is more flexible. For example, where *discretionary* is indicated, *controlled* may be considered more suitable by Council, or vice versa.

Table A3.2 Example of relationships between Resource Consent Category, Building Importance Category, fault Recurrence Interval Class and Fault Complexity for Greenfield sites, based on the MfE Active Fault Guidelines (Kerr et al. 2003).

Greenfield Sites					
PAKARAE FAULT (based on fault Recurrence Interval Class II, >2000 years to ≤3500 years)					
Building Importance Category	**1**	**2a**	**2b**	**3**	**4**
Fault Complexity	**Resource Consent Category**				
Well defined and well-defined extended	Permitted	*Non-Complying*	*Non-Complying*	*Non-Complying*	Prohibited
Distributed and uncertain constrained	Permitted	*Discretionary*	*Non-Complying*	*Non-Complying*	Non-Complying
Uncertain poorly constrained	Permitted	*Controlled*	*Discretionary*	*Non-Complying*	Non-Complying
REPONGAERE FAULT (based on fault Recurrence Interval Class III, >3500 years to ≤5000 years)					
Building Importance Category	**1**	**2a**	**2b**	**3**	**4**
Fault Complexity	**Resource Consent Category**				
Well defined and well-defined extended	Permitted	Permitted*	*Non-Complying*	*Non-Complying*	Non-Complying
Distributed and uncertain constrained	Permitted	Permitted	*Discretionary*	*Discretionary*	Non-Complying
Uncertain poorly constrained	Permitted	Permitted	*Discretionary*	*Discretionary*	Non-Complying

Notes:

* Indicates that the Resource Consent Category is permitted but could be controlled or discretionary, given that the fault location is well-defined.

Italics: The use of italics indicates that the Resource Consent Category of these categories is more flexible. For example, where *discretionary* is indicated, *controlled* may be considered more suitable by Council, or vice versa.

Table A3.3 Recommended actions for the Fault Awareness Areas generated in this study. From Barrell et al. (2015) and Langridge et al. (2021).

<table>
<tr><th rowspan="2">Proposed Activity</th><th colspan="3">Recommended Actions</th></tr>
<tr><td>For FAA categories:
• definite (well expressed)
• definite (moderately expressed)
• likely (well expressed)
• likely (moderately expressed)
with RI Class I, II or III
(<5000 years)</td><td>For FAA categories:
• definite (well expressed)
• definite (moderately expressed)
• likely (well expressed)
• likely (moderately expressed)
with RI Class IV, V or VI
(>5000 years)</td><td>For all other FAA categories:
• definite (not expressed)
• likely (not expressed)
• possible
with no RI Class</td></tr>
<tr><td>Single residential dwelling (BIC 2a and 2b in part)</td><td colspan="3">Permitted activity.</td></tr>
<tr><td>Normal structures and structures not in other categories (BIC 2b, apart from single dwellings)</td><td colspan="2">Consideration of the surface fault-rupture hazard should be a specific assessment matter if resource consent for a new structure is required for some other reason.
Site-specific investigation, including detailed fault mapping at 1:35,000 or better and appropriate mitigation measures for the accurately mapped fault (e.g. setback or engineering measures).</td><td>Permitted activity.</td></tr>
<tr><td>Important or critical structures (BIC 3 and 4)</td><td colspan="3">Consideration of the surface fault-rupture hazard should be a specific assessment matter if resource consent for a new structure is required for some other reason.
Site-specific investigation, including detailed fault mapping at 1:35,000 or better and appropriate mitigation measures determined for the accurately mapped fault (e.g. set-back or engineering measures).</td></tr>
<tr><td>New subdivision (excluding minor boundary adjustments)</td><td colspan="2">Consideration of the surface fault-rupture hazard should be a specific assessment matter.
Site-specific investigation, including detailed fault mapping at 1:35,000 or better and appropriate mitigation measures for the accurately mapped fault (e.g. setback or engineering measures).</td><td>Permitted activity.</td></tr>
<tr><td>Plan Changes</td><td colspan="3">Consideration of the surface fault-rupture hazard should be a specific assessment matter.
Site-specific investigation, including detailed fault mapping at 1:35,000 or better and appropriate mitigation measures for the accurately mapped fault (e.g. setback or engineering measures).</td></tr>
</table>

www.gns.cri.nz

Principal Location

1 Fairway Drive, Avalon
Lower Hutt 5010
PO Box 30368
Lower Hutt 5040
New Zealand
T +64-4-570 1444
F +64-4-570 4600

Other Locations

Dunedin Research Centre
764 Cumberland Street
Private Bag 1930
Dunedin 9054
New Zealand
T +64-3-477 4050
F +64-3-477 5232

Wairakei Research Centre
114 Karetoto Road
Private Bag 2000
Taupo 3352
New Zealand
T +64-7-374 8211
F +64-7-374 8199

National Isotope Centre
30 Gracefield Road
PO Box 30368
Lower Hutt 5040
New Zealand
T +64-4-570 1444
F +64-4-570 4657